

UNCLASSIFIED

AD 414107

DEFENSE DOCUMENTATION CENTER

FOR

SCIENTIFIC AND TECHNICAL INFORMATION

CAMERON STATION, ALEXANDRIA, VIRGINIA



UNCLASSIFIED

NOTICE: When government or other drawings, specifications or other data are used for any purpose other than in connection with a definitely related government procurement operation, the U. S. Government thereby incurs no responsibility, nor any obligation whatsoever; and the fact that the Government may have formulated, furnished, or in any way supplied the said drawings, specifications, or other data is not to be regarded by implication or otherwise as in any manner licensing the holder or any other person or corporation, or conveying any rights or permission to manufacture, use or sell any patented invention that may in any way be related thereto.

AD414107

**The Propagation at Short Ranges of Elastic Waves from
an Impulsive Source at a Liquid-Solid Interface - The
Fluid-Two Layer Solid System,**

NAVY MINE DEFENSE LAB PANAMA CITY FL

AUG 1963

U. S. NAVY MINE DEFENSE LABORATORY
PANAMA CITY, FLORIDA

IN REPLY REFER TO:
Code 712

From: Commanding Officer and Director, U. S. Navy Mine Defense Laboratory,
Panama City, Florida
To: DISTRIBUTION LIST

Subj: NAVMINDEFLAB Unclassified Report 206; information concerning

1. The accompanying report presents the results of an investigation designed to study the pressure field produced at short ranges by an impulsive sound source near a fluid-layered solid interface. Report 195 has shown that a theory is available which can predict the pressure response in the stated problem when the bottom is homogeneous. The present report contains an extension of the theory to a transmission system consisting of a fluid over a layered solid. Experimental data obtained in a model are presented to substantiate the theoretical results. The solution to the problem studied in this investigation should prove useful in practical studies concerning low-frequency sound propagation near the ocean floor.

2. This material is presented for information only.

R.T. Miller

R. T. MILLER

DDC Availability Notice
Qualified requesters may obtain copies
of this report from DDC.

TABLE OF CONTENTS

	<u>Page No.</u>
LIST OF ILLUSTRATIONS	2
LIST OF SYMBOLS	4
SUMMARY	7
INTRODUCTION.	9
MATHEMATICAL PRESSURE RESPONSE DERIVATION FOR THE TWO-LAYER BOTTOM MODEL.	9
DISCUSSION OF THEORETICAL RESULTS	23
EXPERIMENTAL RESULTS.	27
EXPERIMENTAL - THEORETICAL COMPARISON AND DISCUSSION.	29
Water - Plexiglas - Plaster Model.	37
Water - Glass - Aluminum Model	41
CONCLUSIONS	43
DIRECTION OF FUTURE WORK.	44
APPENDIX A - DERIVATION OF THE REFLECTION COEFFICIENTS A(q) and N(q)	49
APPENDIX B - THE REFRACTION AND REFLECTION ARRIVALS	55
APPENDIX C - EXPERIMENTAL INSTRUMENTATION	67
REFERENCES.	69

LIST OF ILLUSTRATIONS

<u>Figure No.</u>		<u>Page No.</u>
1	The Assumed Model	10
2	The 11 Displacement Potentials	11
3	Conditions under which Stoneley Waves can Exist at a Solid-Solid Interface with $\frac{\lambda_1}{\mu_1} = \frac{\lambda_2}{\mu_2} = 1$	28
4	Conditions under which Stoneley Waves can Exist at a Solid-Solid Interface with $\lambda_1 = \lambda_2 = \infty$	28
5	Experimental Pressure Response for a Water-Plexiglas-Plaster Model	30 - 34
6	Experimental Pressure Response for a Water-Glass-Aluminum Model	35 - 36
7	Travel Time Versus Range Curves for the Stoneley Arrivals	40
8	Theoretical Pressure Response Curves for Three Representative Real Ocean Bottoms	45 - 47
B1	The Liquid-Solid Interface	55
B2	The $P_1P_2P_1$, $P_1S_2P_1$, $P_1P_2P_3P_2P_1$, and $P_1S_2S_3S_2P_1$ Refraction Arrivals	56
B3	The $P_1S_2P_3S_2P_1$ and $P_1P_2S_3P_2P_1$ Refraction Arrivals	56
B4	The $P_1P_2P_3S_2P_1$ and $P_1P_2S_3S_2P_1$ Refraction Arrivals	57
B5	The $P_1S_2P_3P_2P_1$ and $P_1S_2S_3P_2P_1$ Refraction Arrivals	57
B6	The P_1RP_1 , $P_1P_2RP_2P_1$, and $P_1S_2RS_2P_1$ Reflection Arrivals	58

LIST OF ILLUSTRATIONS (CONT'D)

<u>Figure No.</u>		<u>Page No.</u>
B7	The $P_1P_2RS_2P_1$ and $P_1S_2RP_2P_1$ Reflection Arrivals	58
B8	The $P_1P_2S_2RS_2P_2P_1$ Refraction-Reflection Arrival	59
B9	The $P_1S_2P_2RP_2S_2P_1$ Refraction-Reflection Arrival	59
B10	Definition of Symbols for the Calculation of the $P_1P_2P_3P_2P_1$ Wave	60
B11	Definition of Symbols for the Calculation of the Arrival Time of the $P_1P_2S_2RS_2P_2P_1$ Arrival	63
C1	Illustration of the Effect of Bonding the Glass and Aluminum Layers	68

LIST OF SYMBOLS

a	compressional sound velocity in upper solid
a'	radical defined in Equation (17)
α	radical defined in Equation (3)
$A, B, C, D, E,$ F, G, M, I, N	complex reflection coefficients defined in Equation (2)
β	radical defined in Equation (3)
b	shear sound velocity in the upper solid
b'	radical defined in Equation (17)
c	compressional sound velocity in the fluid
c'	$\frac{1}{q}$
$D(u)$	denominator of last expression in Equation (21)
$\epsilon_1, \epsilon_2, \epsilon_3, \epsilon_4$	complex expressions defined in Equations (9), (10), (11), (12)
$\Xi_1, \Xi_2, \Xi_3, \Xi_4$	complex expressions defined in Equations (13), (14), (15), (16)
δ_1	radical present in denominator of Equation (20)
g	compressional sound velocity in the lower solid
g'	radical defined in Equation (17)
γ	variable defined as $\cos \theta$
Γ	variable defined as $\frac{1}{c} \cos \theta$
H	source-interface separation

LIST OF SYMBOLS (CONT'D)

\bar{H}	unit step function
J	thickness of solid layer
K_1	ratio of compressional velocities of fluid and upper solid
K_2	ratio of compressional velocity of fluid and shear velocity of solid
k	shear velocity of lower solid
k'	radical defined in Equation (17)
\mathcal{L}	Laplace transform symbol
μ, λ	the Lamé constants
n	parameter defined by Equation (18)
N_1, N_2, N_3	complex expressions defined by Equations (6), (7), (8)
v_1, v_2, v_3	expressions introduced in the transformation from du to $d\tau_i$ -- see Equation (28)
ω	angular frequency of a plane harmonic wave
p_o^f, p_1^f, p_2^f	pressure responses in the fluid due to (1) source in an infinite fluid, (2) contributions due to the fluid-solid interface, and (3) contributions due to the solid-solid interface.
$P_1, P_2, P_1^*, \text{etc.}$	notation employed for denoting wave arrivals
P_o	undetermined constant
$\varphi_o^f, \varphi_1^f, \varphi_2^f$	displacement potentials in the fluid due to (1) source in an infinite fluid, (2) contributions due to the fluid-solid interface, and (3) contributions due to the solid-solid interface.
$\varphi_1^{s_1}, \varphi_2^{s_1}, \varphi_3^{s_1}$	displacement potentials in the upper solid--defined in Figure 2.
$\psi_1^{s_1}, \psi_2^{s_1}, \psi_3^{s_1}$	

LIST OF SYMBOLS (CONT'D)

$\phi_1^{s_2}, \psi_1^{s_2}$	displacement potentials in the lower solid--defined in Figure 2.
q	integration variable defined as $\frac{1}{c} \sin \theta$
Q_0	undetermined constant
r_0	source-detector separation
r_1	first image-detector separation
$\rho^f, \rho_1^{s_1}, \rho_2^{s_2}$	densities of the fluid, upper solid, and lower solid
s	Laplace transform parameter
t	real time
τ_1, τ_2, τ_3	integration variables defined by Equation (27)
θ	angle between the z-axis and the normal to the plane wave
u^{**}	integration variable defined as $u = cq$
v	tangential displacement
w	normal displacement
W	expression defined by Equation (5)
x, y, z	the cartesian coordinates in this problem

*The code employed in identifying the arrivals is explained in Appendix B. In general, subscripts 1, 2, and 3 refer to the fluid, first solid, and second solid, respectively; while P, S, and R refer to compressional waves, shear waves, and a reflection, respectively. For example, $P_1 P_2 S_3 P_2 P_1$ refers to an arrival that has traveled from the source to the first interface as a compressional wave, and from the first interface to the second interface as a compressional wave. Then, it is critically refracted at the second interface and travels along this interface with the shear velocity of the lower solid. This critically refracted wavefront generates a new compressional wave back into the upper solid, which then travels through the water as a compressional wave to the detector.

**u is also used as a displacement in Appendix A. No confusion should result from this dual usage.

SUMMARY

The problem of the prediction of the exact pressure field produced at close ranges by an impulsive sound source near a fluid-layered solid interface is considered. A theory is developed that should accurately provide arrival time data and exact pressure response waveform data for a model consisting of an explosive acoustic source in a fluid overlying a two-layered solid. Experimental pressure response curves have been obtained with the use of models and are presented to support the theoretical development. Although the final results of the theory are not at present in closed form, it is anticipated that such results should be possible in the near future.

The method of Cagniard, which is a Laplace transform technique, is utilized in the mathematical development. Although this type of derivation becomes quite complicated, it is worthwhile because it enables one to obtain expressions describing exact pressure response waveforms that are in closed form; that is requiring no further integrations.

It was shown in a previous paper¹ that for low-frequency sound transmission near the ocean floor, the bottom cannot be considered as a liquid because of the possibility of surface waves occurring at the bottom interface. These waves are attenuated in a direction normal to the interface, and hence are not important at high frequencies or large distances from the interface.

The experimental data presented was obtained in a model using previously developed experimental techniques.¹ The sound source was a coaxial spark gap and the hydrophone, or detector, was a small ultrasonic probe. Model solids included plexiglas, plaster, flint glass, aluminum, and lead.

It is concluded that the theoretical approach of Cagniard appears to be quite applicable to problems of the type presented here. The extended theory developed in this report is accurate in predicting most expected arrivals at short ranges in the experimental model. It is anticipated that further theoretical development will provide exact waveform data. Except for rare situations, it is found that surface waves cannot exist at real solid-solid interfaces. Additional surface waves appear to exist at the fluid-solid interface because of reflections from lower solid-solid interfaces. The results obtained in this

investigation continue to illustrate the large errors in wave propagation predictions near an interface that can occur when the ocean bottom is considered to be a fluid. It is hoped that further work on problems of this type will eventually permit the prediction of the exact pressure field produced by an explosive source near a real ocean floor.

INTRODUCTION

A theory recently published by Strick² has been found to give reasonable accuracy in prediction of the pressure fields at short ranges from an impulsive sound source near a fluid-homogeneous solid interface. However, the assumption of the homogeneous solid greatly restricts the application of this theory. When considering low frequencies it is difficult, if not impossible to find an ocean bottom that is homogeneous down to a depth of at least one wavelength, the point at which surface wave effects can usually be neglected. If the mean frequency under consideration is 15 cycles, a typical hard bottom ($a = 7500$ ft/sec) would have to be homogeneous down to a depth of about 500 feet.

Hence, this report is intended to extend the theory advanced by Strick to a model consisting of a fluid overlying a two-layer solid. Although the final result of the extended theory is not in closed form, it is developed to a point that one can predict and identify the elastic wave arrivals occurring in the pressure response curves obtained from the experimental model.

Pekeris³ presented the normal mode theory for explosive sound transmission in three liquid layers in 1948, and this problem has been further investigated by Officer⁴ and Press and Ewing⁵. McLeroy⁶ has published a complex image theory for near-field, low frequency propagation in shallow water overlying a many-layered bottom, but it is not valid for the problem to be considered here.

MATHEMATICAL PRESSURE RESPONSE DERIVATION* FOR THE TWO-LAYER BOTTOM MODEL

The geometry of the problem is presented in Figure 1. As in Reference 1, the liquid is considered to be semi-infinite in extent.

*To the best of our knowledge this derivation has not been made elsewhere.

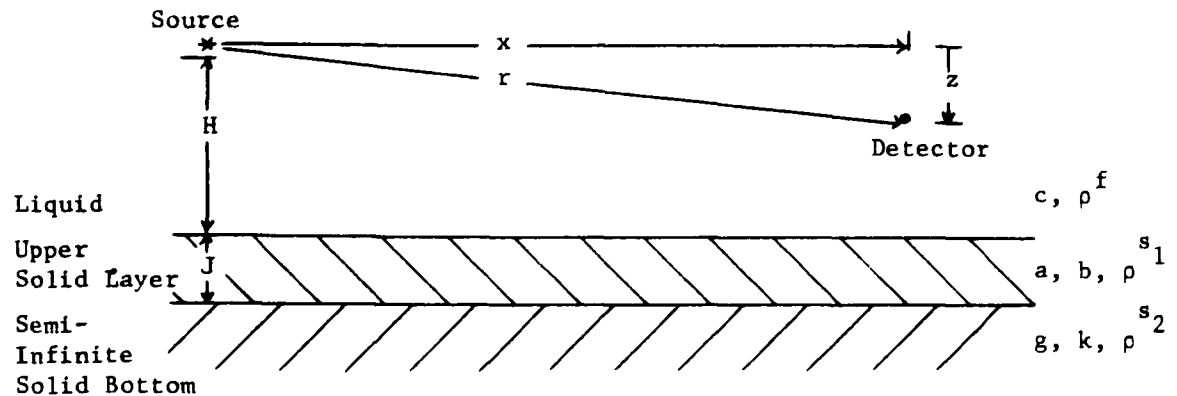


FIGURE 1. THE ASSUMED MODEL

It will be seen that the derivation for this extended problem will closely follow that given by Strick² in his original derivation for a liquid-homogeneous solid model. A simplified version of this derivation, along with a number of added explanatory comments, can be found in Reference (1). It will be assumed that the reader is familiar with at least one of the aforementioned papers.

Figure 2 serves to identify the 11 displacement potentials that will be considered in this problem. It will be assumed that any waves existing after two reflections from the lower (solid-solid) interface can be neglected. For many situations this is not a good assumption, but it is not so unreasonable when one realizes that the predominant waveform, the surface wave, dies out exponentially with distance normal to the interface. The introduction of the middle layer into the problem has made a rigorous solution of the problem by the potential technique difficult, as there are now an infinite number of potentials that should be considered. As in the homogeneous bottom problem, the pressure response will be obtained for a delta-excited line source, instead of an explosive point source.

φ_0^f is the displacement potential due to the line sound source in an infinite fluid. φ_1^f represents the displacement potential due to energy propagated back into the liquid because of the presence of the fluid-solid interface. Likewise, φ_2^f is the displacement potential representing energy propagated back into the fluid because of the presence of the solid-solid interface. As shown in Appendix A of Reference 1, two potentials are necessary to describe the wave propagation in an infinite

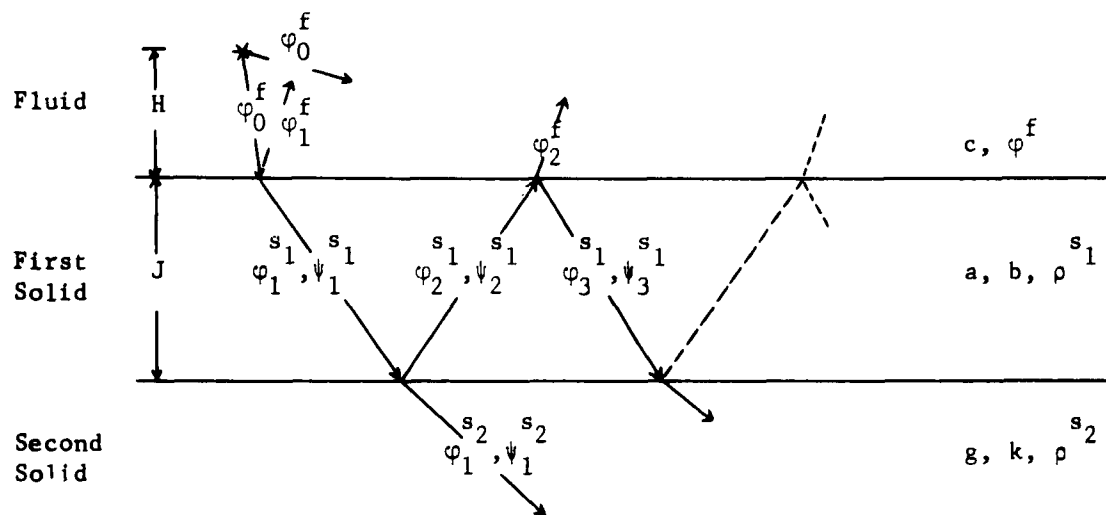


FIGURE 2. THE 11 DISPLACEMENT POTENTIALS

solid medium. Hence, potentials such as $\varphi_1^{s_1}$ and $\psi_1^{s_1}$ are necessary in the solid.

The displacement potential in an infinite fluid due to a harmonic line source is given by ¹

$$\varphi_0^f(x, z; e^{i\omega t}) = Q_0 \int_{-\infty}^{\infty} \frac{e^{-i\omega(\Gamma z + qx)} d q e^{i\omega t}}{\Gamma}, \quad (1)$$

where

$$Q_0 = \frac{P_0}{2i\rho_f \omega^2}, \quad \Gamma = \left(\frac{1}{c^2} - q^2\right)^{\frac{1}{2}},$$

and

$$q = \frac{1}{c} \sin \theta$$

the angle θ is defined as the angle between the vertical z -axis and the wave vector associated with each elementary plane wavefront assumed in obtaining Equation (1). The other potentials in the problem are given by Equations (2a-j), where $A(q)$ through $N(q)$ represent reflection and transmission coefficients which will be evaluated shortly:

$$\varphi_1^f(x, z; e^{i\omega t}) = Q_0 \int_{-\infty}^{\infty} \frac{A(q) e^{-i\omega[\Gamma(2H-z) + qx]} dq e^{i\omega t}}{\Gamma} \quad (2a)$$

$$\varphi_1^s(x, z; e^{i\omega t}) = Q_0 \int_{-\infty}^{\infty} \frac{B(q) e^{-i\omega[\frac{1}{a^2} - q^2]^{\frac{1}{2}} z + qx]} dq e^{i\omega t}}{\Gamma} \quad (2b)$$

$$\psi_1^s(x, z; e^{i\omega t}) = Q_0 \int_{-\infty}^{\infty} \frac{C(q) e^{-i\omega[\frac{1}{b^2} - q^2]^{\frac{1}{2}} z + qx]} dq e^{i\omega t}}{\Gamma} \quad (2c)$$

$$\varphi_2^s(x, z; e^{i\omega t}) = Q_0 \int_{-\infty}^{\infty} \frac{D(q) e^{-i\omega[\frac{1}{a^2} - q^2]^{\frac{1}{2}} (2H + 2J - z) + qx]} dq e^{i\omega t}}{\Gamma} \quad (2d)$$

$$\psi_2^s(x, z; e^{i\omega t}) = Q_0 \int_{-\infty}^{\infty} \frac{E(q) e^{-i\omega[\frac{1}{b^2} - q^2]^{\frac{1}{2}} (2H + 2J - z) + qx]} dq e^{i\omega t}}{\Gamma} \quad (2e)$$

$$\varphi_3^s(x, z; e^{i\omega t}) = Q_0 \int_{-\infty}^{\infty} \frac{F(q) e^{-i\omega[\frac{1}{a^2} - q^2]^{\frac{1}{2}} (2J + z) + qx]} dq e^{i\omega t}}{\Gamma} \quad (2f)$$

$$\psi_3^s(x, z; e^{i\omega t}) = Q_0 \int_{-\infty}^{\infty} \frac{G(q) e^{-i\omega[\frac{1}{b^2} - q^2]^{\frac{1}{2}} (2J + z) + qx]} dq e^{i\omega t}}{\Gamma} \quad (2g)$$

$$\varphi_1^s(x, z; e^{i\omega t}) = Q_0 \int_{-\infty}^{\infty} \frac{M(q) e^{-i\omega[\frac{1}{a^2} - q^2]^{\frac{1}{2}} z + qx]} dq e^{i\omega t}}{\Gamma} \quad (2h)$$

$$\psi_1^s(x, z; e^{i\omega t}) = Q_0 \int_{-\infty}^{\infty} \frac{I(q) e^{-i\omega \left[\left(\frac{1}{k^2} - q^2 \right)^{\frac{1}{2}} z + qx \right]}}{\Gamma} dq e^{i\omega t} \quad (2i)$$

$$\varphi_2^f(x, z; e^{i\omega t}) = Q_0 \int_{-\infty}^{\infty} \frac{N(q) e^{-i\omega [\Gamma(2H + 2J - z) + qx]}}{\Gamma} dq e^{i\omega t} \quad (2j)$$

The boundary conditions are:

- (1) The normal stresses are continuous at both interfaces.
- (2) The normal displacements are continuous at both interfaces.
- (3) The tangential stresses are zero at the liquid-solid interface and continuous at the solid-solid interface.
- (4) The tangential displacements are continuous at the solid-solid interface.

These boundary conditions give 10 boundary equations which can be used to evaluate the 10 unknowns, A, B, C, D, E, F, G, M, I, and N. Actually, as we are only interested in the response in the fluid, it is only necessary to determine A(q) and N(q). The details of the derivation of these quantities are given in Appendix A. As expected, A(q), or A(u) with a change of variables, is unchanged from the similar reflection coefficient occurring in the original fluid - homogeneous solid derivation and is given by

$$A(u) = \frac{\gamma(K_2^2 - 2u^2)^2 + 4u^2\alpha\gamma\beta - \frac{\rho f}{\rho s_1} K_2^4 \alpha}{\gamma(K_2^2 - 2u^2)^2 + 4u^2\alpha\gamma\beta + \frac{\rho f}{\rho s_1} K_2^4 \alpha}, \quad (3)$$

where

$$\alpha = (K_1^2 - u^2)^{\frac{1}{2}},$$

$$\beta = (K_2^2 - u^2)^{\frac{1}{2}},$$

$$\gamma = (1 - u^2)^{\frac{1}{2}},$$

$$K_1 = c/a,$$

$$K_2 = c/b,$$

$$u = cq,$$

c = compressional sound velocity in the fluid,

a = compressional sound velocity in the first solid,

and b = shear sound velocity in the first solid.

$N(q)$ is considerably more complicated than $A(q)$ and is given by

$$N(q) = \frac{N_1 e^{-2i\omega J(a' - \Gamma)} + N_2 e^{-2i\omega J(b' - \Gamma)} + N_3 e^{-i\omega J(a' + b' - 2\Gamma)}}{W(\Xi_4 \epsilon_3 - \Xi_3 \epsilon_4)}, \quad (4)$$

where:

$$W = \rho^f + 4\rho^s_1 b^2 q^2 b' \Gamma + \frac{\rho^s_1 \Gamma (1 - 2b^2 q^2)^2}{a'} \quad (5)$$

$$N_1 = [(1 - 2b^2 q^2)^2 (4\rho^f \Gamma) (\Xi_1 \epsilon_4 - \Xi_4 \epsilon_1)] \div [a' \frac{\rho^f}{\rho s_1} + \Gamma n] \quad (6)$$

$$N_2 = [16 \rho^f \Gamma b^4 q^2 a' b' (\Xi_2 \epsilon_3 - \epsilon_2 \Xi_3)] \div [a' \frac{\rho^f}{\rho s_1} + \Gamma n] \quad (7)$$

$$N_3 = [-8\rho^f \Gamma b^2 q (1 - 2b^2 q^2)] [b' (\Xi_1 \epsilon_3 - \epsilon_1 \Xi_3) + a' (\Xi_2 \epsilon_4 - \Xi_4 \epsilon_2)] \div [a' \frac{\rho^f}{\rho s_1} + \Gamma n] \quad (8)$$

$$\epsilon_1 = \left\{ \left[2\rho^s_1 b^2 q a' - \frac{\rho^s_2 q}{k'} (1 - 2k^2 q^2) \right] + \left[2k^2 q^2 + \frac{\rho^s_1}{s_2} (1 - 2b^2 q^2) \right] \cdot \right. \\ \left. [-2\rho^s_2 k^2 g' q + \frac{\rho^s_2 q}{k'} (1 - 2k^2 q^2)] \right\} \quad (9)$$

$$\epsilon_2 = \left\{ \left[\rho^{s_1} (1 - 2b^2 q^2) - \frac{\rho^{s_2} b'}{k} (1 - 2k^2 q^2) \right] + \left[-2k^2 q b' + \frac{2\rho^{s_1}}{\rho s_2} b^2 b' q \right] \cdot \right. \\ \left. \left[2\rho^{s_2} k^2 g' q - \frac{\rho^{s_2} q}{k} (1 - 2k^2 q^2) \right] \right\} \quad (10)$$

$$\epsilon_3 = \left\{ \left[-2\rho^{s_1} b^2 a' q - \rho^{s_2} \frac{q}{k'} (1 - 2k^2 q^2) \right] + \left[\frac{\rho^{s_1}}{\rho s_2} (1 - 2b^2 q^2) + 2k^2 q^2 \right] \cdot \right. \\ \left. \left[-2\rho^{s_2} k^2 g' q + \frac{\rho^{s_2} q}{k'} (1 - 2k^2 q^2) \right] \right\} \quad (11)$$

$$\epsilon_4 = \left\{ \left[\rho^{s_1} (1 - 2b^2 q^2) + \frac{b' \rho^{s_2}}{k'} (1 - 2k^2 q^2) \right] + \left[\frac{-2\rho^{s_1}}{\rho s_2} b^2 q b' + 2k^2 q b' \right] \cdot \right. \\ \left. \left[2\rho^{s_2} k^2 g' q - \frac{\rho^{s_2} q}{k'} (1 - 2k^2 q^2) \right] \right\} \quad (12)$$

$$\Xi_1 = \left\{ \left(\frac{-q^2}{k'} - a' \right) + \left(g' + \frac{q^2}{k'} \right) \left[2k^2 q^2 + \frac{\rho^{s_1}}{\rho s_2} (1 - 2b^2 q^2) \right] \right\} \quad (13)$$

$$\Xi_2 = \left\{ \left(q - \frac{b' q}{k'} \right) + \left(g' + \frac{q^2}{k'} \right) \left[2k^2 q b' - \frac{2\rho^{s_1}}{\rho s_2} b^2 b' q \right] \right\} \quad (14)$$

$$\Xi_3 = \left\{ \left(a' - \frac{q^2}{k'} \right) + \left(g' + \frac{q^2}{k'} \right) \left[\frac{\rho^{s_1}}{\rho s_2} (1 - 2b^2 q^2) + 2k^2 q^2 \right] \right\} \quad (15)$$

$$\Xi_4 = \left\{ \left(q + \frac{b' q}{k'} \right) + \left(g' + \frac{q^2}{k'} \right) \left[\frac{2\rho^{s_1}}{\rho s_1} b^2 q b' - 2k^2 q b' \right] \right\} \quad (16)$$

$$\begin{aligned}
a' &= \left(\frac{1}{a^2} - q^2 \right)^{\frac{1}{2}} \\
b' &= \left(\frac{1}{b^2} - q^2 \right)^{\frac{1}{2}} \\
g' &= \left(\frac{1}{g^2} - q^2 \right)^{\frac{1}{2}} \\
k' &= \left(\frac{1}{k^2} - q^2 \right)^{\frac{1}{2}}
\end{aligned} \tag{17}$$

g = compressional sound velocity in the lower solid

k = shear sound velocity in the lower solid

$$n = (1 - 2b^2 q^2)^2 + 4b^4 q^2 a' b' \tag{18}$$

The total displacement potential in the fluid is given by

$$\varphi^f = \varphi_o^f + \varphi_1^f + \varphi_2^f ,$$

and the total fluid pressure response is

$$p^f = p_o^f + p_1^f + p_2^f .$$

φ_o^f , and hence p_o^f , is unchanged from the original homogeneous solid problem. For an impulsive type sound source,

$$p_o^f(x, z; \delta) = \frac{P_o c \bar{H}(t - \frac{r_o}{c})}{r_o \left(\frac{c^2 t^2}{r_o^2} - 1 \right)^{\frac{1}{2}}} \tag{19}$$

where

$$r_o = (x^2 + z^2)^{\frac{1}{2}} ,$$

\bar{H} = the unit step-function,

and P_o is an undetermined constant depending on the strength of the sound source. Likewise, since φ_1^f is unchanged, p_1^f is unchanged, and is given by

$$p_1^f(x, z; \delta) = \frac{P_0 c}{r_1} (I) \left[\frac{A(u)}{\delta} \right] \bar{H}(t - t_{P_1 P_2 P_1}) \quad (20)$$

where

$$r_1 = \left[x^2 + (2H - z)^2 \right]^{\frac{1}{2}},$$

$$\delta = \left[1 - \left(\frac{ct}{r_1} \right)^2 \right]^{\frac{1}{2}},$$

and

$$t_{P_1 P_2 P_1} = \frac{x}{a} + \frac{(2H - z)}{c} \left[1 - \frac{c^2}{a^2} \right]^{\frac{1}{2}}.$$

The evaluation of this expression for three ranges of t and for $b < c$ (Case 1) or $b > c$ (Case 2) gives:

$$(a) \text{ Case 1: } t_{P_1 P_2 P_1} \leq t \leq \frac{r_1}{c}, \text{ Case 2: } t_{P_1 P_2 P_1} \leq r \leq r_{P_1 S_2 P_1}$$

$$p_1^f(x, z; \delta) = \frac{2 \frac{\rho^f}{s_1} K_2^4 P_0 c}{r_1 \delta} \left[\frac{\gamma (K_2^2 - 2u^2)^2 (u^2 - K_1^2)^{\frac{1}{2}}}{\gamma^2 (K_2^2 - 2u^2)^4 - \alpha^2 (4u^2 \beta \gamma + \frac{\rho^f}{s_1} K_2^4)} \right],$$

where

$$t_{P_1 S_2 P_1} = \frac{x}{b} + \frac{(2H - z)}{c} \left(1 - \frac{c^2}{b^2} \right)^{\frac{1}{2}}.$$

$$(b) \text{ Case 1: } p_1^f \equiv 0, \text{ Case 2: } t_{P_1 S_2 P_1} \leq t \leq \frac{r_1}{c}$$

$$p_1^f(x, z; \delta) = \frac{2 \frac{\rho^f}{s_1} K_2^4 P_0 c}{r_1 \delta} \cdot \frac{\gamma (u^2 - K_1^2)^{\frac{1}{2}} f(u)}{\gamma^2 f(u)^2 - \alpha^2 \left(\frac{\rho^f}{s_1} \right)^2 K_2^8}$$

where

$$f(u) = (K_2^2 - 2u^2)^2 - 4u^2(u^2 - K_1^2)^{\frac{1}{2}} (u^2 - K_2^2)^{\frac{1}{2}}.$$

$$(c) \text{ Case 1: } t \geq \frac{r_1}{c}, \text{ Case 2: } t \geq \frac{r_1}{c}$$

$$\rho_1^f(x, z; \delta) = \frac{P_o c}{r_1 |\delta|} \frac{|\gamma|^2 |f(u)|^2 - K_2^8 \left(\frac{\rho_f}{s_1}\right)^2 |\alpha|^2}{|D|^2} \quad (21)$$

where

$$D(u) = \gamma f(u) + \left(\frac{\rho_f}{s}\right) K_2^4 \alpha.$$

It is now necessary to find $p_2^f(x, z; \delta)$, the pressure response in the fluid due to contributions from the solid-solid boundary when the sound source is impulsive. It was shown above that the integral expression for p_2^f is

$$p_2^f(x, z; e^{i\omega t}) = \frac{P_o}{2i} \int_{-\infty}^{\infty} \frac{N e^{-i\omega[\Gamma(2H + 2J - z) + qx]} dqe^{i\omega t}}{\Gamma} \quad (22)$$

Or, using Equation (4)

$$\begin{aligned} p_2^f(x, z; e^{i\omega t}) &= \frac{P_o}{2i} \int_{-\infty}^{\infty} \frac{N_1 e^{-i\omega[\Gamma(2H - z) + 2Ja' + qx]} dqe^{i\omega t}}{\Gamma W(\Xi_4 \epsilon_3 - \Xi_3 \epsilon_4)} \\ &+ \frac{P_o}{2i} \int_{-\infty}^{\infty} \frac{N_2 e^{-i\omega[\Gamma(2H - z) + 2Jb' + qx]} dqe^{i\omega t}}{\Gamma W(\Xi_4 \epsilon_3 - \Xi_3 \epsilon_4)} \\ &+ \frac{P_o}{2i} \int_{-\infty}^{\infty} \frac{N_3 e^{-i\omega[\Gamma(2H - z) + J(a' + b') + qx]} dqe^{i\omega t}}{\Gamma W(\Xi_4 \epsilon_3 - \Xi_3 \epsilon_4)} \end{aligned}$$

$$= [p_2^f(x, z; e^{i\omega t})]_1 + [p_2^f(x, z; e^{i\omega t})]_2 + [p_2^f(x, z; e^{i\omega t})]_3 \quad (23)$$

The expression for the s-multiplied Laplace transform of the p_2^f contribution to the total pressure response due to a step-function excitation of the source can now be obtained by replacing $i\omega$ by s and dropping the $e^{i\omega t}$ in Equation (23). This is a technique used in filter analysis and brief explanations can be found elsewhere.^{1,2}

Thus,

$$\begin{aligned} \overline{p_2^f}(x, z; e^{i\omega t}) &= \frac{P_0}{2i} \int_{-\infty}^{\infty} \frac{N_1 e^{-s[\Gamma(2H - z) + 2Ja' + qx]} dq}{\Gamma W(\Xi_4 \epsilon_3 - \Xi_3 \epsilon_4)} \\ &+ \frac{P_0}{2i} \int_{-\infty}^{\infty} \frac{N_1 e^{-s[\Gamma(2H - z) + 2Jb' + qx]} dq}{\Gamma W(\Xi_4 \epsilon_3 - \Xi_3 \epsilon_4)} \\ &+ \frac{P_0}{2i} \int_{-\infty}^{\infty} \frac{N_3 e^{-s[\Gamma(2H - z) + J(a' + b') + qx]} dq}{\Gamma W(\Xi_4 \epsilon_3 - \Xi_3 \epsilon_4)} \end{aligned} \quad (24)$$

The s-multiplied Laplace transform of a sum is the sum of the transforms of the individual components, so it is possible to separate the problem into:

$$\overline{p_2^f}(x, z; \text{step}) = [\overline{p_2^f}(x, z; \text{step})]_1 + [\overline{p_2^f}(x, z; \text{step})]_2 + [\overline{p_2^f}(x, z; \text{step})]_3 ,$$

where

$$\begin{aligned} (\overline{p_2^f})_1 &= \frac{P_0}{2i} \int_{-\infty}^{\infty} \frac{N_1 e^{-\frac{s}{c}[(2H - z) \gamma + 2cJa' + ux]} du}{\Gamma W(\Xi_4 \epsilon_3 - \Xi_3 \epsilon_4)} , \\ (\overline{p_2^f})_2 &= \frac{P_0}{2i} \int_{-\infty}^{\infty} \frac{N_2 e^{-\frac{s}{c}[(2H - z) \gamma + 2cJb' + ux]} du}{\Gamma W(\Xi_4 \epsilon_3 - \Xi_3 \epsilon_4)} , \end{aligned}$$

$$\overline{(p_2^f)_3} = \frac{P_0}{2i} \int_{-\infty}^{\infty} \frac{N_3 e^{-\frac{s}{c}[(2H-z)\gamma + cJ(a' + b') + ux]}}{\Gamma W(\Xi_4 \epsilon_3 - \Xi_3 \epsilon_4)} du, \quad (25)$$

and

$$u = cq, \quad \Gamma = \frac{\gamma}{c}.$$

To obtain the inverse s-multiplied Laplace transform it will be necessary to have an expression of the form

$$\overline{P}(x, z; \text{step}) = (\text{Constant}) \int_0^{\infty} [fn(u)] e^{-s\tau} d\tau. \quad (26)$$

Then, using the derivative rule for s-multiplied Laplace transforms,

$$\mathcal{L}(f'(t)) = s \mathcal{L}(f(t)) - s f(0),$$

and the fact that the delta-response is the derivative of the step-response, it will be possible to obtain the delta-function excitation pressure response in a closed form:

$$p(x, z; \text{delta}) = \text{Constant} [fn(u)]$$

So, to reduce Equation (25) to three equations of the form of Equation (26) it is necessary to define τ_1 , τ_2 , and τ_3 :

$$\tau_1 = \frac{(2H-z)}{c} (1-u^2)^{\frac{1}{2}} + 2J\left(\frac{1}{a^2} - \frac{u^2}{c^2}\right)^{\frac{1}{2}} + \frac{ux}{c} \quad (27a)$$

$$\tau_2 = \frac{(2H-z)}{c} (1-u^2)^{\frac{1}{2}} + 2J\left(\frac{1}{b^2} - \frac{u^2}{c^2}\right)^{\frac{1}{2}} + \frac{ux}{c} \quad (27b)$$

$$\tau_3 = \frac{(2H-z)}{c} (1-u^2)^{\frac{1}{2}} + J\left[\frac{1}{b^2} - \frac{u^2}{c^2}\right]^{\frac{1}{2}} + \left(\frac{1}{a^2} - \frac{u^2}{c^2}\right)^{\frac{1}{2}} + \frac{ux}{c} \quad (27c)$$

τ_1 , τ_2 and τ_3 each contain at least one term that is not present in the transformation to τ_1 in the homogeneous bottom problem. The transformation in that case is

$$\tau_1(\text{Homogeneous bottom}) = \frac{(2H - z)}{c} (1 - u^2)^{\frac{1}{2}} + \frac{ux}{c}.$$

It was relatively easy to determine u as a function of τ_1 in that case, but for the current problem this becomes much more difficult. On the other hand, it is still possible to obtain an expression for du as a function of $d\tau_i$ and u .

From Equations (27a), (27b) and (27c), after a substitution of previously defined quantities, it is found that:

$$du = \frac{d\tau_1}{\left[\frac{-(2H - z)u}{\gamma c} - \frac{2Ju}{a'^2 c^2} + \frac{x}{c} \right]} \quad (28a)$$

$$du = \frac{d\tau_2}{\left[\frac{-(2H - z)u}{\gamma c} - \frac{2Ju}{b'^2 c^2} + \frac{x}{c} \right]} \quad (28b)$$

$$du = \frac{d\tau_3}{\left[\frac{-(2H - z)u}{\gamma c} - \frac{Ju}{c^2} \left(\frac{1}{a'} + \frac{1}{b'} \right) + \frac{x}{c} \right]} \quad (28c)$$

Then,

$$\begin{aligned} \overline{f}_2(x, z; \text{step}) = & \frac{P_0}{2i} \int_{c\tau_1} \frac{N_1 e^{-s\tau_1} d\tau_1}{\gamma W v_1 (\Xi_4 \epsilon_3 - \Xi_3 \epsilon_4)} \\ & + \frac{P_0}{2i} \int_{c\tau_2} \frac{N_2 e^{-s\tau_2} d\tau_2}{\gamma W v_2 (\Xi_4 \epsilon_3 - \Xi_3 \epsilon_4)} + \frac{P_0}{2i} \int_{c\tau_3} \frac{N_3 e^{-s\tau_3} d\tau_3}{\gamma W v_3 (\Xi_4 \epsilon_3 - \Xi_3 \epsilon_4)}, \quad (29) \end{aligned}$$

where v_i is defined by the denominators of Equations (28a), (28b) and (28c).

The problem has been reduced to expressions of the form

$$\left[\overline{p_2^f(x, z; \text{step})} \right] = (\text{Constant}) \int_{c_{\tau_i}} \left[f_{n_i}(u) \right] e^{-s\tau_i} d\tau_i \quad .$$

(i = 1, 2, 3)

But, since

$$s \left[\overline{p_2^f(x, z; \text{step})} \right] = \overline{p_2^f(x, z; \text{delta})}$$

as was discussed previously,

$$\left[\overline{p_2^f(x, z; \text{delta})} \right]_i = s(\text{Constant}) \int_{c_{\tau_i}} \left[f_{n_i}(u) \right] e^{-s\tau_i} d\tau_i$$

(i = 1, 2, 3) (30)

The right-hand side of this expression is in the form of an s-multiplied Laplace transform, except for the fact that the limits on the integral are not proper. Once the integral over the contour c_{τ_i} is changed to an integral over $\tau_i = 0$ to $\tau_i = \infty$, expression (30) will be of suitable form to take the inverse Laplace transform. The problem will then be in a closed form requiring no further integration. This transform to a proper form of integral is complicated by the presence of a large number of poles and branch points, and by the fact that u cannot be found as an explicit function of τ_i . Work is continuing at the present time on this transformation. But, there is still a large amount of extremely useful information in the present integral form of the delta response. The closed form solution is desired to theoretically predict the exact waveform of the various elastic waves, but this waveform can also be found experimentally in a model. This experimental problem then reduces to identifying the type of wave with the waveform. The present form of the theory is sufficient to make this identification.

DISCUSSION OF THEORETICAL RESULTS

In the fluid - homogeneous bottom problem Strick found that each elastic wave could be predicted by the existence of poles and branch points in his expression for the total pressure response. Thus, the indicated procedure at this point is to search for similar singularities in Equation (29), noting that in general p_o^f and p_1^f have already predicted the existence of P, S, direct, reflected, Rayleigh and Stoneley waves due to the presence of the water-solid interface.^{1,2}

Branch points are present in the denominator of Equation (29) at $u = \pm \frac{c}{a}, \pm \frac{c}{b}, \pm \frac{c}{g},$ and $\pm \frac{c}{k}.$ * When these values for u are inserted into the expressions for τ_i , it is found that:

$$\tau_1(u = \frac{c}{a}) = \frac{(2H - z)}{c} (1 - \frac{c^2}{a^2})^{\frac{1}{2}} + \frac{x}{a} \equiv t_{P_1 P_2 P_1} \quad (31a)$$

$$\tau_1(u = \frac{c}{b}) = \frac{(2H - z)}{c} (1 - \frac{c^2}{b^2})^{\frac{1}{2}} + 2J(\frac{1}{2} - \frac{1}{b^2})^{\frac{1}{2}} + \frac{x}{b} \equiv t_{P_1 S_2 P_2 R P_2 S_2 P_1} \quad (31b)$$

$$\tau_1(u = \frac{c}{g}) = \frac{(2H - z)}{c} (1 - \frac{c^2}{g^2})^{\frac{1}{2}} + 2J(\frac{1}{2} - \frac{1}{g^2})^{\frac{1}{2}} + \frac{x}{g} \equiv t_{P_1 P_2 P_3 P_2 P_1} \quad (31c)$$

$$\tau_1(u = \frac{c}{k}) = \frac{(2H - z)}{c} (1 - \frac{c^2}{k^2})^{\frac{1}{2}} + 2J(\frac{1}{2} - \frac{1}{k^2})^{\frac{1}{2}} + \frac{x}{k} \equiv t_{P_1 P_2 S_3 P_2 P_1} \quad (31d)$$

* In the transformation from u to τ_i , the γ factor should drop out and

be replaced by $\delta = (1 - \frac{c^2 t^2}{r_1^2})^{\frac{1}{2}}$, representing a reflected wave from

the liquid-solid interface. See the original paper by Strick² for an elaboration on this point.

$$\tau_2(u = \frac{c}{a}) = \frac{(2H - z)}{c} (1 - \frac{c^2}{a^2})^{\frac{1}{2}} + 2J(\frac{1}{b^2} - \frac{1}{a^2})^{\frac{1}{2}} + \frac{x}{a} \equiv t_{P_1 P_2 S_2 R S_2 P_2 P_1} \quad (31e)$$

$$\tau_2(u = \frac{c}{b}) = \frac{(2H - z)}{c} (1 - \frac{c^2}{b^2})^{\frac{1}{2}} + \frac{x}{b} \equiv t_{P_1 S_2 P_1} \quad (31f)$$

$$\tau_2(u = \frac{c}{g}) = \frac{(2H - z)}{c} (1 - \frac{c^2}{g^2})^{\frac{1}{2}} + 2J(\frac{1}{b^2} - \frac{1}{g^2})^{\frac{1}{2}} + \frac{x}{g} \equiv t_{P_1 S_2 P_3 S_2 P_1} \quad (31g)$$

$$\tau_2(u = \frac{c}{k}) = \frac{(2H - z)}{c} (1 - \frac{c^2}{k^2})^{\frac{1}{2}} + 2J(\frac{1}{b^2} - \frac{1}{k^2})^{\frac{1}{2}} + \frac{x}{k} \equiv t_{P_1 S_2 S_3 S_2 P_1} \quad (31h)$$

$$\tau_3(u = \frac{c}{a}) = \frac{(2H - z)}{c} (1 - \frac{c^2}{a^2})^{\frac{1}{2}} + J(\frac{1}{b^2} - \frac{1}{a^2})^{\frac{1}{2}} + \frac{x}{a} \quad (31i)$$

$$\tau_3(u = \frac{c}{b}) = \frac{(2H - z)}{c} (1 - \frac{c^2}{b^2})^{\frac{1}{2}} + J(\frac{1}{a^2} - \frac{1}{b^2})^{\frac{1}{2}} + \frac{x}{b} \quad (31j)$$

$$\begin{aligned} \tau_3(u = \frac{c}{g}) &= \frac{(2H - z)}{c} (1 - \frac{c^2}{g^2})^{\frac{1}{2}} + J\left[\left(\frac{1}{b^2} - \frac{1}{g^2}\right)^{\frac{1}{2}} + \left(\frac{1}{a^2} - \frac{1}{g^2}\right)^{\frac{1}{2}}\right] + \frac{x}{g} \\ &\equiv t_{P_1 S_2 P_3 P_2 P_1} = t_{P_1 P_2 P_3 S_2 P_1} \end{aligned} \quad (31k)$$

$$\begin{aligned} \tau_3(u = \frac{c}{k}) &= \frac{(2H - z)}{c} (1 - \frac{c^2}{k^2})^{\frac{1}{2}} + J\left[\left(\frac{1}{b^2} - \frac{1}{k^2}\right)^{\frac{1}{2}} + \left(\frac{1}{a^2} - \frac{1}{k^2}\right)^{\frac{1}{2}}\right] + \frac{x}{k} \\ &\equiv t_{P_1 P_2 S_3 S_2 P_1} = t_{P_1 S_2 S_3 P_2 P_1} \end{aligned} \quad (31l)$$

Appendix B contains geometrical derivations for the travel times of the critically refracted and the reflected - critically refracted arrivals that are to be expected in this problem. An analysis of these travel time expressions will show that the geometrical travel times are given by equations identical to those given by Equations (31), except that no geometrical arrivals can be found to correspond to Equations (31i) and (31j). Also, an analysis of the experimental results will show that no arrivals are present corresponding to those described by (31i) or (31j). Note that when (31i) is not complex, (31j) is complex, and when (31i) is complex, (31j) is not complex. Hence, arrivals corresponding to (31i) and (31j) could never exist simultaneously.

Poles exist in Equation (29) corresponding to the vanishing of v_1, v_2, v_3, W , or $(\Xi_4 \epsilon_3 - \Xi_3 \epsilon_4)$. v_1, v_2 and v_3 are given by the denominators of Equations (28a, b, c) respectively. It is hypothesized that when the value of u that corresponds to the vanishing of v_i is substituted into the corresponding τ_i equation, the τ_i equation will give the travel time of an arrival that has been refracted at the fluid-solid interface, reflected at the solid-solid interface, and again refracted at the fluid-solid interface. Geometrically, the approach necessary to determine a travel time for such a reflected wave consists of using an iterative process to find a reflected travel path that satisfies Snell's law for a given set of dimensional and elastic parameters. It will be seen that the two methods give identical results, so it is concluded that the mathematical approach hypothesized is valid.

From Equation (5),

$$W = \rho^f + 4 \frac{s_1}{\rho} b^4 q^2 b' \Gamma + \rho^s (1 - 2b^2 q^2)^2 \frac{\Gamma}{a'} \\ = \frac{\rho^s}{\alpha K_2^4} \left[\gamma (K_2^2 - 2u^2)^2 + 4\gamma u^2 \alpha \beta + \frac{\rho^f}{s_1} K_2^4 \alpha \right] \quad (32)$$

The term in brackets in Equation (32) is exactly the denominator in Equation (3). In the liquid-homogeneous solid problem the vanishing of the denominator of Equation (3) defined the phase velocity of the Stoneley interface wave. Hence, Equation (32) simply predicts a Stoneley wave traveling along the fluid-solid boundary. Using the data from Table 1 and the Stoneley wave charts⁷, it is found that for a water-plexiglas interface, Equation (32) vanishes for a value of u corresponding to a Stoneley velocity of 1.03×10^5 centimeters per second.

The expression $(\Xi_4 \epsilon_3 - \Xi_3 \epsilon_4)$ contains terms depending on the elastic constants of both solid media, and it is hypothesized that the vanishing of this term describes the propagation of a Stoneley surface wave at the interface of the two solid media. It seems likely that the expression $(\Xi_4 \epsilon_3 - \Xi_3 \epsilon_4)$ should reduce to the equation obtained by Stoneley^{8,10} to describe the propagation of a surface wave at the interface of two solid media.

If $(\Xi_4 \epsilon_3 - \Xi_3 \epsilon_4)$ is multiplied by $-kq^{-6} \rho^{s_2}$ and the resulting expression is simplified, it is found that

$$\begin{aligned}
 -k'c'^6 \rho^{s_2} (\Xi_4 \epsilon_3 - \Xi_3 \epsilon_4) = & \\
 & c'^4 \left[(\rho^{s_2})^2 c'^2 a'b' + (\rho^{s_1})^2 c'^2 g'k' + \rho^{s_1} \rho^{s_2} c'^2 a'k' + \rho^{s_1} \rho^{s_2} c'^2 b'g' \right. \\
 & \left. + (\rho^{s_2})^2 - 2\rho^{s_1} \rho^{s_2} + (\rho^{s_1})^2 \right] \\
 & + c'^2 \left[4\rho^{s_1} \rho^{s_2} b^2 c'^2 a'b' - 4(\rho^{s_2})^2 k^2 c'^2 a'b' - 4(\rho^{s_1})^2 b^2 c'^2 g'k' \right. \\
 & \left. + 4\rho^{s_1} \rho^{s_2} k^2 c'^2 g'k' + 4\rho^{s_1} \rho^{s_2} k^2 + 4\rho^{s_1} \rho^{s_2} b^2 - 4(\rho^{s_1})^2 b^2 - 4(\rho^{s_2})^2 k^2 \right] \\
 & + \left[c'^4 a'b'g'k' (4(\rho^{s_1})^2 b^4 - 8\rho^{s_1} \rho^{s_2} b^2 k^2 + 4(\rho^{s_2})^2 k^4) + 4(\rho^{s_1})^2 c'^2 b^4 a'b' \right. \\
 & - 8\rho^{s_1} \rho^{s_2} b^2 c'^2 k^2 a'b' + 4(\rho^{s_2})^2 k^4 c'^2 a'b' + 4(\rho^{s_2})^2 k^4 c'^2 g'k' \\
 & + 4(\rho^{s_1})^2 b^4 c'^2 g'k' - 8\rho^{s_1} \rho^{s_2} k^2 b^2 c'^2 g'k' + 4(\rho^{s_2})^2 k^4 \\
 & \left. + 4(\rho^{s_1})^2 b^4 - 8\rho^{s_1} \rho^{s_2} k^2 b^2 \right],
 \end{aligned}$$

where $c' = \frac{1}{q}$.

(33)

Now, let

$$a' = \pm \frac{1}{c'} A_1, \quad b' = \pm \frac{1}{c'} B_1, \quad g' = \pm \frac{1}{c'} A_2, \quad \text{and} \quad k' = \pm \frac{1}{c'} B_2.$$

Then

$$\begin{aligned}
 -k'c' \rho^s \left(\Xi_4 \epsilon_3 - \Xi_3 \epsilon_4 \right) &= c'^4 \left[(\rho^{s1} - \rho^{s2})^2 - (\rho^{s1} A_2 + \rho^{s2} A_1) (\rho^{s1} B_2 + \rho^{s2} B_1) \right] \\
 + 2Kc' \left[\rho^{s1} A_2 B_2 - \rho^{s2} A_1 B_1 - \rho^{s1} + \rho^{s2} \right] &+ K^2 \left[A_1 B_1 - 1 \right] (A_2 B_2 - 1) , \\
 \text{where } K &= 2(\rho^{s1} b^2 - \rho^{s2} k^2) .
 \end{aligned} \tag{34}$$

This is exactly the equation describing the Stoneley wave that was obtained by Stoneley in his original solid-solid problem.³

Scholte⁹ has investigated Equation (34) in an attempt to determine the conditions under which Stoneley waves can exist at a solid-solid interface. He found that they can exist at the interface only under a set of extremely stringent conditions. The results of Scholte's investigation are presented in Figures 3 and 4. Stoneley waves can exist only in the shaded regions. μ_1 and λ_1 are the Lamé constants of the solids. These conditions are in fact so stringent that it is difficult to conceive of a model that can satisfy them. It is necessary to consider a radical model like plexiglas over lead in order to formulate a system that will contain Stoneley arrivals that originate at a solid-solid interface. When such a model is considered experimentally, the Stoneley velocity is so slow that multiple reflections occurring at the boundaries of the experimental system makes the identification of a "Stoneley-type" wave impossible. Certainly, a model such as plexiglas over lead, where the densities differ by a factor of ten, should not be found in nature.

EXPERIMENTAL RESULTS

The apparatus used in the experimental phase of this project was quite similar to that utilized in previous work with the homogeneous bottom. A brief description of the instrumentation and model facility can be found in Appendix C of this paper. The major experimental problem encountered in the layered bottom extension was a question concerning the bonding of the solid layers. As described in Appendix C, it was found that for our very smooth and flat surfaces the bonding of the layers was not important. The two models used in the experimental phase of the project were water - plexiglas - plaster and water - glass - aluminum. The elastic and physical parameters of these materials are given in Table 1.

(Text Continued on Page 29)

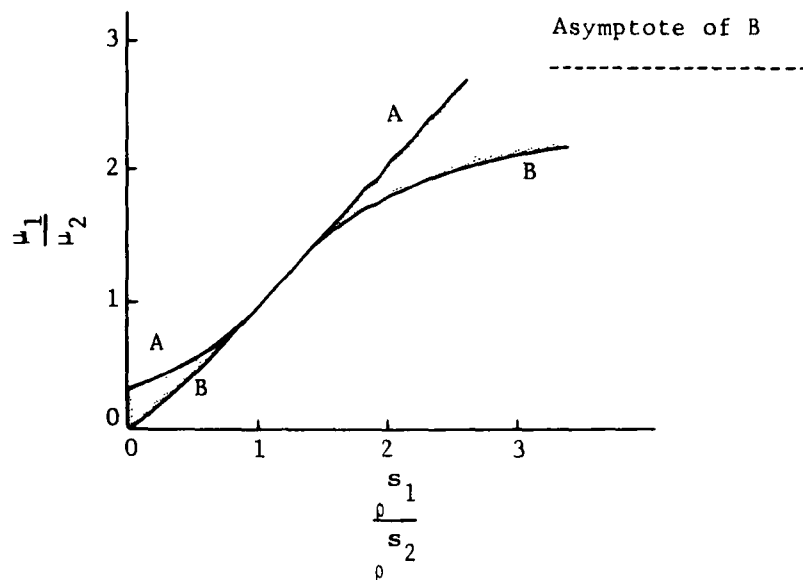


FIGURE 3. CONDITIONS UNDER WHICH STONELEY WAVES CAN EXIST AT A
SOLID-SOLID INTERFACE WITH $\frac{\lambda_1}{\mu_1} = \frac{\lambda_2}{\mu_2} = 1$

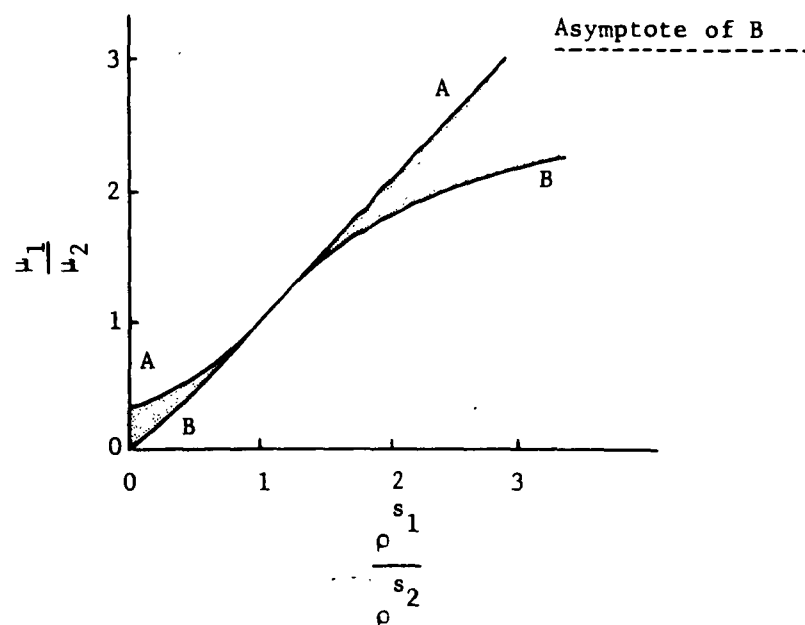


FIGURE 4. CONDITIONS UNDER WHICH STONELEY WAVES CAN EXIST AT A
SOLID-SOLID INTERFACE WITH $\lambda_1 = \lambda_2 = \infty$

TABLE 1

ELASTIC PARAMETERS IN THE MODEL

Material	Compressional Velocity (cm/sec)	Shear Velocity (cm/sec)	Density (gm/cm ³)	Thickness (cm)
Water	1.46×10^5	-	1.00	∞ (20.0)
Plexiglas	2.62×10^5	1.30×10^5	1.17	3.81
Plaster	2.83×10^5	1.80×10^5	1.89	∞ (24.0)
Glass	3.30×10^5	1.56×10^5	3.50	1.27
Aluminum	5.26×10^5	2.95×10^5	2.70	∞ (20.9)

Figures 5 and 6 are typical pressure response versus time curves obtained for the two models. The amplitudes are relative and travel times are accurate to ± 1.0 microsecond. The noted wave identifications will be discussed in the next section.

EXPERIMENTAL - THEORETICAL COMPARISON AND DISCUSSION

The large number of elastic wave arrivals occurring in a short time period in this problem prohibit all of the theoretical arrivals to be identified from any one experimental photograph. In an attempt to experimentally identify as many of the arrivals as possible, two widely varying models were chosen: water-plexiglas-plaster, and water-glass-aluminum. Primary attention will be directed toward the water-plexiglas-plaster model, although several aspects of the results obtained from the water-glass-aluminum model will be discussed. Because of the limiting assumption that all arrivals experiencing two or more reflections from the solid-solid interface may be neglected, it should not be expected that all experimental arrivals will be predicted theoretically.

(Text Continued on Page 37)

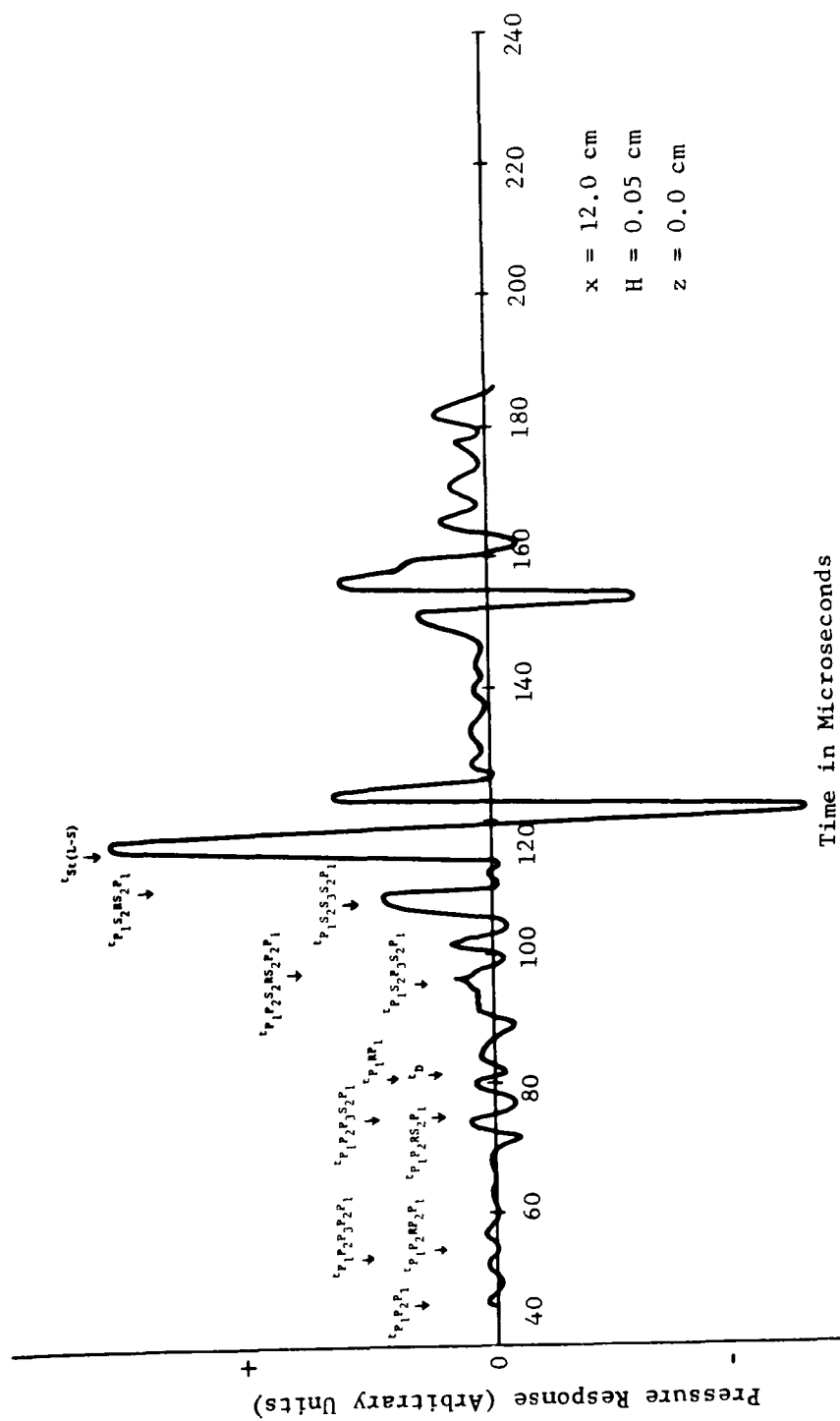


FIGURE 5b. EXPERIMENTAL PRESSURE RESPONSE FOR A WATER-PLEXIGLAS-PLASTER MODEL.

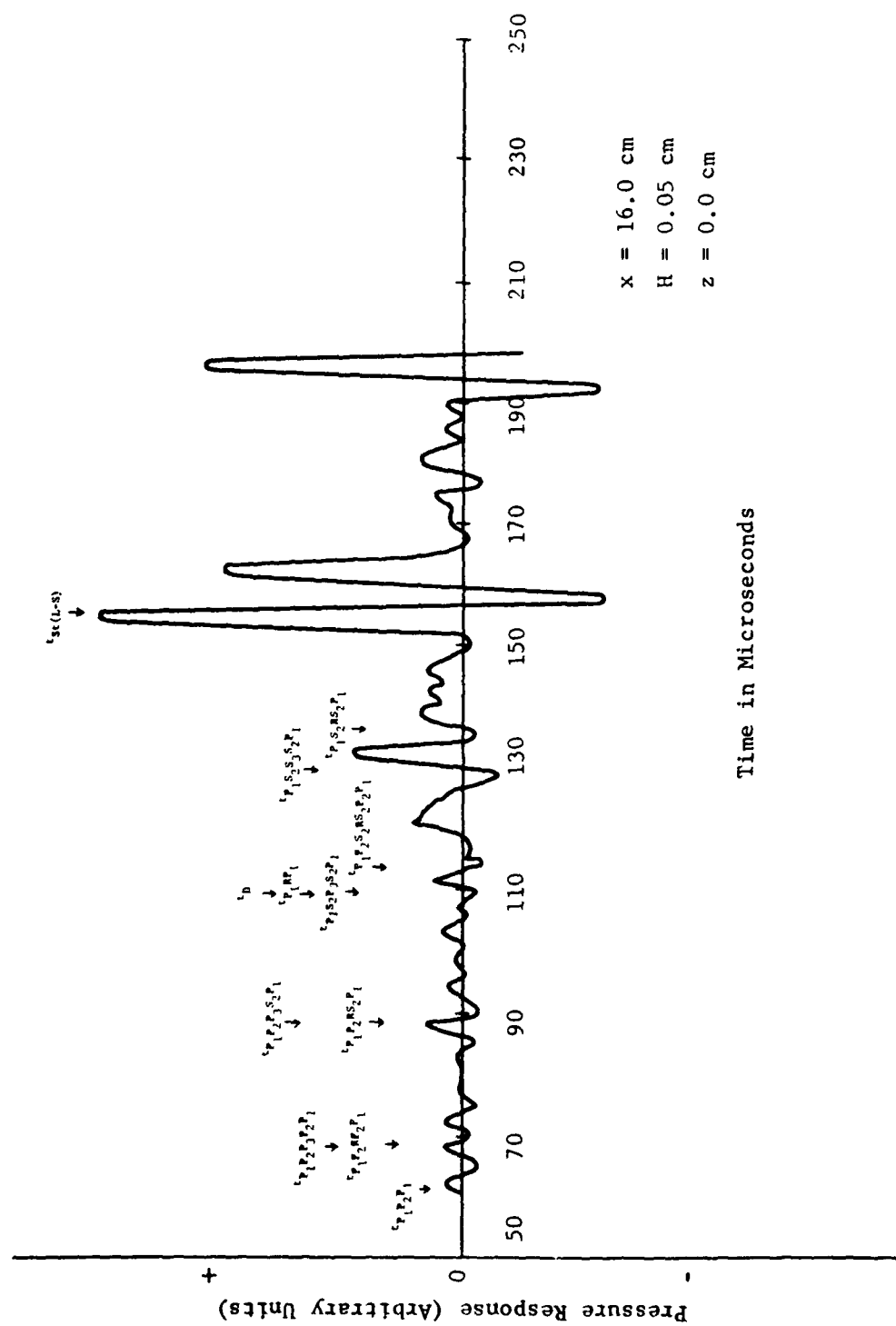
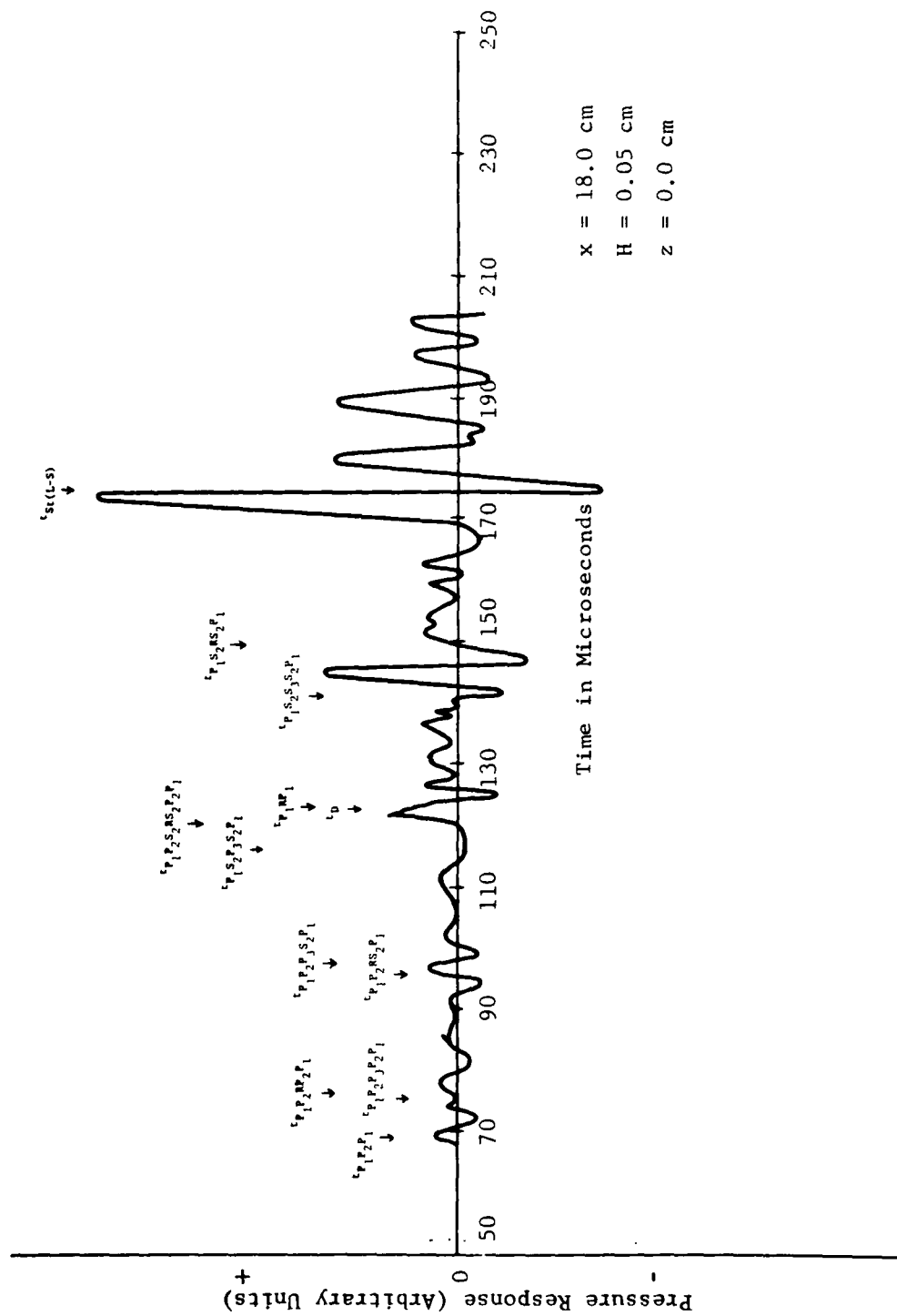


FIGURE 5d. EXPERIMENTAL PRESSURE RESPONSE FOR A WATER-PLEXIGLAS-PLASTER MODEL



WATER - PLEXIGLAS - PLASTER MODEL

Table 2 contains the computed theoretical travel times in the water-plexiglas-plaster model when $H = 0.05$ centimeters, and $z = 0.0$ centimeters. These theoretical arrival times have been included in Figure 5 so that they might easily be compared with the experimental results.

It has been shown previously² that a Rayleigh wave or a critically refracted shear wave cannot be propagated when the shear velocity of the solid at the fluid-solid interface is less than the compressional sound velocity of the fluid. Hence, since such a relationship between elastic constants is present in the water - plexiglas - plaster model, the $P_1S_2P_1$ and Rayleigh arrivals do not exist. It can be shown in a manner similar to that utilized above that the $P_1P_2S_3P_2P_1$, $P_1P_2S_3S_2S_1$, and $P_1S_2P_2RP_2S_2P_1$ arrivals may not exist in this model. Also, when the elastic parameters of the two solids are analyzed with respect to Scholte's criteria for the existence of surface waves at a solid-solid interface (Figures 3 and 4), it can be seen that such an arrival is not possible for this model.

Referring to Figure 5a, it can be seen that for this range of 10 centimeters, the first arrival (38 microseconds) appears to be the $P_1P_2P_1$ wave, the next arrival (45 microseconds) is the $P_1P_2P_3P_2P_1$ arrival, and the third arrival (49 microseconds) appears to be the $P_1P_2RP_2P_1$ arrival. Two small peaks appear at 58 and 72 microseconds which have not been identified. At 69 microseconds there is a relatively strong arrival which appears to be a superposition of the $P_1P_2RS_2P_1$, $P_1S_2P_3P_2P_1$, direct, and P_1RP_1 arrivals. Following the direct arrival there is a region of small oscillations which was also noted in the fluid-homogeneous solid problem. This oscillation is again related to the fact that we have an explosive type point source instead of a delta-excited line source as the theory assumed. The direct pulse is about 4 microseconds long and the reflected (P_1RP_1) pulse occurs soon after the beginning of the direct pulse. The P_1RP_1 arrival experiences a large phase change when it is reflected at this range, so strong interference should be expected in this region of the pressure response curve as the arrival times for the direct and P_1RP_1 arrivals are almost the same. The arrival at 90 microseconds is due to the $P_1S_2P_3S_2P_1$ and $P_1P_2S_2RS_2P_2P_1$ arrivals.

A very large pressure increase begins at about 97 microseconds and reaches a peak at about 100 microseconds. Three arrivals, the $P_1S_2S_3S_2P_1$, $P_1S_2RS_2P_1$, and Stoneley (Liquid-Solid) are predicted in this region.

(Text Continued on Page 39)

TABLE 2

THEORETICAL ARRIVAL TIMES FOR THE WATER - PLEXIGLAS - PLASTER
MODEL (H = 0.05 cm, z = 0.0 cm, x = Variable)

Wave Type	Arrival Time in Microseconds				
	x = 10.0 cm	x = 12.0 cm	x = 14.0 cm	x = 16.0 cm	x = 18.0 cm
t(D)	68.5	82.2	95.8	109.5	123.3
t(P ₁ RP ₁)	68.5	82.2	95.8	109.5	123.3
t(P ₁ P ₂ P ₁)	38.8	46.4	54.0	61.6	69.3
t(P ₁ S ₂ P ₁)	-	-	-	-	-
t(P ₁ P ₂ P ₃ P ₂ P ₁)	46.8	53.9	60.9	67.9	75.2
t(P ₁ S ₂ S ₃ S ₂ P ₁)	96.4	107.5	118.5	129.5	140.8
t(P ₁ S ₂ P ₃ S ₂ P ₁)	88.7	95.5	102.5	109.6	116.8
t(P ₁ P ₂ S ₃ P ₂ P ₁)	-	-	-	-	-
t(P ₁ P ₂ P ₃ S ₂ P ₁)	67.6	74.7	81.7	88.8	96.0
t(P ₁ P ₂ S ₃ S ₂ P ₁)	-	-	-	-	-
t(P ₁ P ₂ RP ₂ P ₁)	48.9	54.2	61.2	68.0	76.0
t(P ₁ S ₂ RS ₂ P ₁)	96.7	109.4	122.6	135.9	149.6
t(P ₁ P ₂ RS ₂ P ₁)	67.5	74.4	81.2	88.9	96.3
t(P ₁ P ₂ S ₂ RS ₂ P ₂ P ₁)	89.6	97.0	104.7	112.4	120.0
t(P ₁ S ₂ P ₂ RP ₂ S ₂ P ₁)	-	-	-	-	-
t(Rayleigh)	-	-	-	-	-
t(Stoneley:Liq.-Sol.)	97.0	116.2	136.0	155.5	174.5
t(Stoneley:Sol.-Sol.)	-	-	-	-	-

Pressure response curves obtained at larger ranges will show that this large peak is primarily due to a Stoneley (Liquid-Solid) arrival. Many of the arrivals occurring after the Stoneley peak are due to reflections disallowed in the theoretical derivation. It will be shown that the large arrival at about 142 microseconds is also a Stoneley (Liquid-Solid) arrival.

The first three arrivals in Figure 5b (range = 12 centimeters) again appear to be the $P_1P_2P_1$, $P_1P_2P_3P_2P_1$, and $P_1P_2RP_2P_1$ arrivals, occurring at 47, 52, and 56 microseconds respectively. The two small arrivals at 63 and 68 microseconds have not been identified. The peak at 75 microseconds is a superposition of the $P_1P_2RS_2P_1$ and $P_1P_2P_3S_2P_1$ arrivals. The direct and reflected (P_1RP_1) arrivals occur at about 82 microseconds, followed by the usual region of oscillations, some of which are relatively large in this pressure response curve. The $P_1P_2S_2RS_2P_2P_1$ and $P_1S_2P_3S_2P_1$ arrivals are predicted at 97 microseconds, but appear to be somewhat distorted. The arrival at 102 microseconds is unexplained. The large arrival with a peak at 108 microseconds is predicted to be the $P_1S_2S_3S_2P_1$ arrival. A weak arrival, possibly the $P_1S_2RS_2P_1$ occurs at 112 microseconds. It must be noted that many of the reflected arrivals have probably experienced phase changes greater than 90 degrees; and hence, these arrivals may be negative rather than positive peaks. The large Stoneley (Liquid-Solid) arrival begins at 114 microseconds and reaches a peak at 117 microseconds. The strong arrival at about 156 microseconds will be identified as a Stoneley (Liquid-Solid) arrival later.

Referring to Figure 5c, it is now seen that the two small arrivals at 63 and 68 microseconds are unidentified. Also, two moderate arrivals at 127 and 130 microseconds are unidentified. Of course, the two predominant waveforms are the Stoneley arrival at 135 microseconds and the other large arrival at 175 microseconds which will be discussed shortly.

Figures 5d and 5e show that the Stoneley arrival continues to be the predominant waveform, although the $P_1S_2S_3S_2P_1$ arrival is beginning to show a rather large amplitude. Several arrivals continue to be unidentified.

Figure 7 shows the travel time versus range curves for the Stoneley (Liquid-Solid) arrival and for the large unidentified arrival that usually occurs about 40 microseconds after the Stoneley arrival. The inverse slopes of these curves represent the velocity with which the waves are traveling. The theoretical Stoneley velocity is 1.03×10^5 centimeters per seconds, while the experimental velocity is

(Text Continued on Page 41)

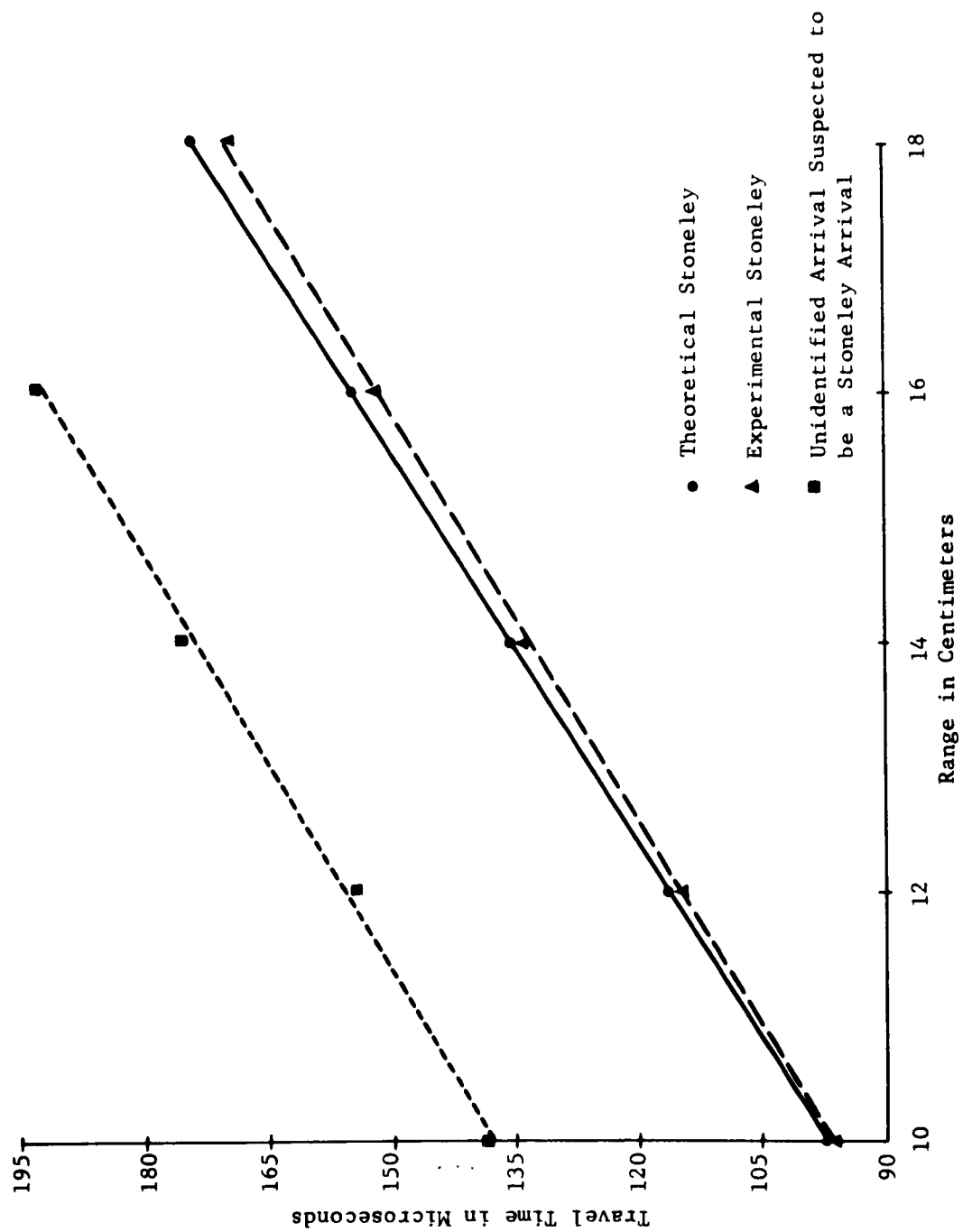


FIGURE 7. TRAVEL TIME VERSUS RANGE CURVES FOR THE STONELEY ARRIVALS

1.09×10^5 centimeters per second. The large unidentified arrival that is suspected to be a Stoneley arrival has a velocity of 1.11×10^5 centimeters per second. Since this velocity is considerably less than the sound velocity in either of the solids, it is strongly indicated that this arrival must be identified as a Stoneley arrival. But, the Stoneley wave is propagated only along the interface (i.e., horizontally) so this latter arrival cannot represent a reflection of the Stoneley wave. The possibility remains that a compressional wave in the fluid could be refracted as it enters the upper solid, reflected at the solid-solid interface, and then strike the fluid-solid interface at such an angle so that it would force the formation of a Stoneley-type arrival. But, if this is the situation, geometrical considerations show that such an arrival could not occur in this model unless the range was greater than 15 centimeters. Thus, the exact reason for the existence of the latter "Stoneley-like" arrival is unknown. It is apparent that further research related to the rather strange physical mechanisms by which surface waves are formed and propagated will be necessary to solve this problem.

WATER - GLASS - ALUMINUM MODEL

The theoretical travel times in the water - glass - aluminum model when $H = 0.5$ centimeters and $z = 0.0$ centimeters are given in Table 3. As before, these theoretical times have been included in Figure 6 so that they might easily be compared with the experimental results.

The first arrival in Figure 6a appears to be due to both the $P_1P_2P_1$ and $P_1P_2P_3P_2P_1$ arrivals. The next two arrivals are due to the $P_1P_2P_3S_2P_1$ and $P_1P_2RS_2P_1$ waves. At about 35 microseconds, the direct arrival occurs, supported by the $P_1S_2P_2RP_2S_2P_1$, Rayleigh, and $P_1S_2P_1$ arrivals. The reflected (P_1RP_1) arrival does not now interfere with the direct arrival as much, as there is almost a 1 microsecond difference in arrival times. The peak occurring at about 41 microseconds is the Stoneley (Liquid-Solid) arrival. No Stoneley (Solid-Solid) arrival can exist in this model. In addition, several of the reflection and refraction arrivals cannot occur, as can be seen in Table 3.

Referring to Figure 6b, the first arrival (26 microseconds) is now the $P_1P_2P_3P_2P_1$ arrival. That is, the arrival that is critically refracted at the solid-solid interface has a shorter travel time than the arrival that is critically refracted at the fluid-solid interface. The arrival at 30 microseconds is evidently due to a superposition of the $P_1P_2P_1$ and $P_1P_2RP_2P_1$ arrivals. The $P_1P_2P_3S_2P_1$ arrival is predicted to occur 31.6 microseconds, but no such arrival is present. The contribution at about $t = 36$ microseconds is due to the $P_1P_2RS_2P_1$ and

(Text Continued on Page 43)

TABLE 3
THEORETICAL ARRIVAL TIMES FOR THE WATER - GLASS - ALUMINUM
MODEL (H = 0.5 cm, z = 0.0 cm, x = Variable)

Wave Type	Arrival Time in Microseconds	
	x = 5.0 cm	x = 7.5 cm
t(D)	34.2	51.3
t(P ₁ RP ₁)	35.0	52.3
t(P ₁ P ₂ P ₁)	21.3	28.9
t(P ₁ S ₂ P ₁)	34.4	50.4
t(P ₁ P ₂ P ₃ P ₂ P ₁)	22.1	26.9
t(P ₁ S ₂ S ₃ S ₂ P ₁)	-	-
t(P ₁ S ₂ P ₃ S ₂ P ₁)	31.6	36.4
t(P ₁ P ₂ S ₃ P ₂ P ₁)	-	-
t(P ₁ P ₂ P ₃ S ₂ P ₁)	26.8	31.6
t(P ₁ P ₂ S ₃ S ₂ P ₁)	-	-
t(P ₁ P ₂ RP ₂ P ₁)	23.3	30.3
t(P ₁ S ₂ RS ₂ P ₁)	40.0	54.0
t(P ₁ P ₂ RS ₂ P ₁)	29.1	36.5
t(P ₁ P ₂ S ₂ RS ₂ P ₂ P ₁)	-	-
t(P ₁ S ₂ P ₂ RP ₂ S ₂ P ₁)	35.7	43.2
t(Rayleigh)	35.0	52.4
t(Stoneley:Liq.-Sol.)	40.0	60.0
t(Stoneley:Sol.-Sol.)	-	-

$P_1S_2P_3S_2P_1$ arrivals. The $P_1S_2P_2R_2S_2P_1$ arrival occurs at 42.5 microseconds, although it is quite weak. Also, a small disturbance at about 40 microseconds is believed to be the $P_1S_2P_1$ arrival. Again, several arrivals support the direct pulse at about 51 microseconds. The Stoneley zero crossing is at 58.8 microseconds, while the Stoneley peak occurs at about 60 microseconds.

CONCLUSIONS

The most important conclusions that can be stated at this time are:

1. The theoretical approach utilized appears to be quite applicable to problems of the type considered here. Arrival time predictions can be obtained with little effort, and exact amplitude data should be available when the mathematical development can be completed.
2. The extended theory developed in this report is accurate in predicting most expected arrivals at short ranges in the experimental model, although several experimental arrivals are received that are not predicted. Further development of the theory, which will give waveform data, should prove useful in determining the origin of these unexpected arrivals.
3. Except for rare situations, Stoneley waves cannot exist at real solid-solid interfaces. It must be emphasized that such waves are theoretically possible under certain conditions, but that these conditions are so stringent that they can be rarely satisfied.
4. An additional Stoneley-type wave appears to exist at the fluid-solid interface because of a reflection from the solid-solid interface, although this cannot be substantiated by a geometrical analysis.
5. The work performed on this phase of the project continues to illustrate the large errors in wave propagation predictions near an interface that can occur when a hard bottom is theoretically considered to be a fluid.
6. Although this paper has considered only a fluid-two layer-solid model, the results are useful when considering other models. The principal contribution to the pressure response waveform obtained in the fluid near a hard bottom will often be the Stoneley wave propagated at the fluid-solid interface, although several such waves may be present if the bottom contains a number of layers.

DIRECTION OF FUTURE WORK

It is apparent that much research remains to be done in the field of elastic wave propagation near an interface. Many questions remain unanswered, as has been noted throughout this report. Certainly, it seems that surface waves must be responsible for a major part of the pressure response when one considers the propagation of low-frequency sound near a hard ocean floor, and hence a thorough understanding of such wave propagation is important.

The problem of elastic wave propagation has been under investigation since before the turn of the century, and research in this field will certainly continue well into the future. Because of the complexity of the mathematics involved in the rigorous solution of any elastic wave propagation problem, many limiting assumptions are almost always necessary. Often it is necessary to accept assumptions that make experimental verification of theoretical results difficult, if not impossible. For this reason, the efforts expended in this field at this Laboratory have been planned so that experimental and theoretical developments go side-by-side. Models are chosen so the theoretical assumptions necessary to solve a specific problem may be experimentally duplicated.

Future endeavors on this project should include:

1. A completion of the mathematical development presented in this report--This will consist of performing the transformation from the variable q to real time, and then programming the results through use of a computer so that pressure response versus time curves can be easily obtained for any system to be considered.
2. Inclusion of the contributions due to reflections from the water-air interface--This will be a mathematical and experimental development quite similar to that presented in this report.
3. Comparison of theoretical and model work with data obtained over a soft bottom for an explosive type sound source--This data is now available and preliminary analysis should begin in the near future. Although most of the model work has been done with rigid materials, it must be stressed that the theory is also applicable to softer bottom materials. Figure 8a, b and c contains pressure response curves for systems consisting of (a) recent sediments, (b) consolidated sediments, and (c) metamorphic rock. It can be seen that Stoneley wave contributions are substantial even for the recent sediment bottom. Since the Stoneley wave is symmetrical, most of the response following the direct arrival can be attributed to it. Hence, an analysis of the available data should show surface wave contributions.

(Text Continued on Page 48)

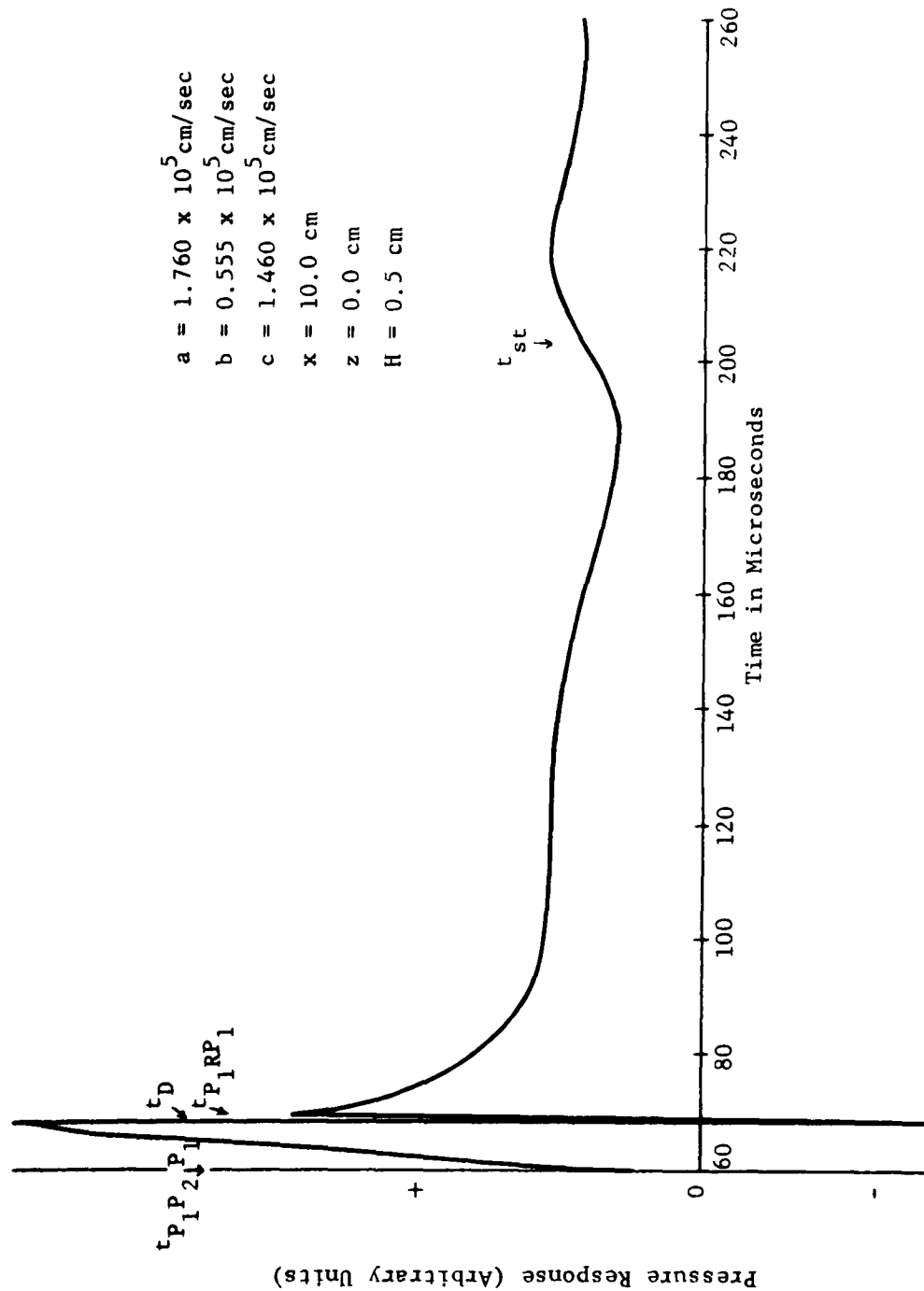


FIGURE 8a. THEORETICAL PRESSURE RESPONSE CURVE FOR A
WATER - RECENT SEDIMENT SYSTEM

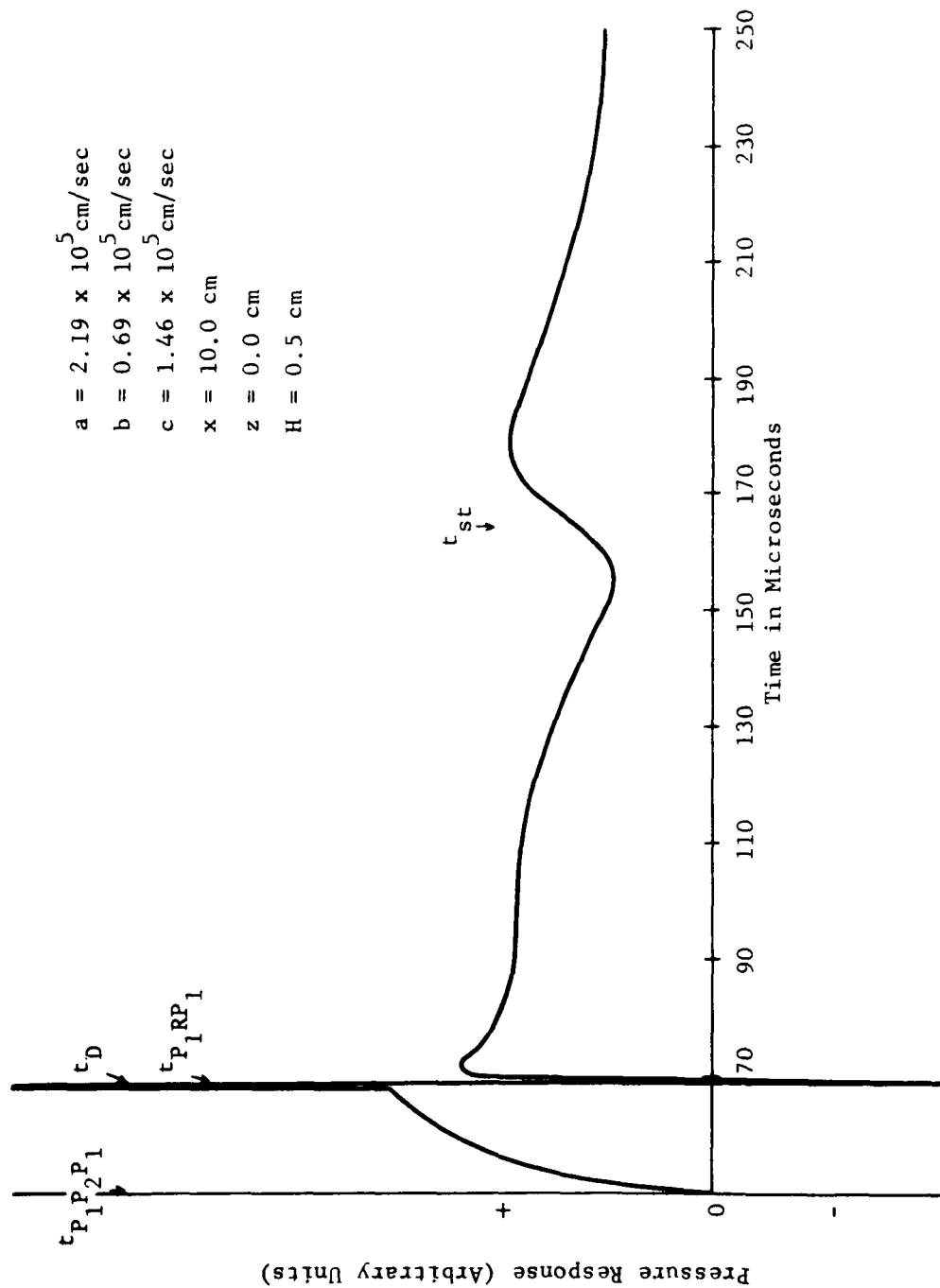


FIGURE 8b. THEORETICAL PRESSURE RESPONSE CURVE FOR A WATER -
CONSOLIDATED SEDIMENT SYSTEM

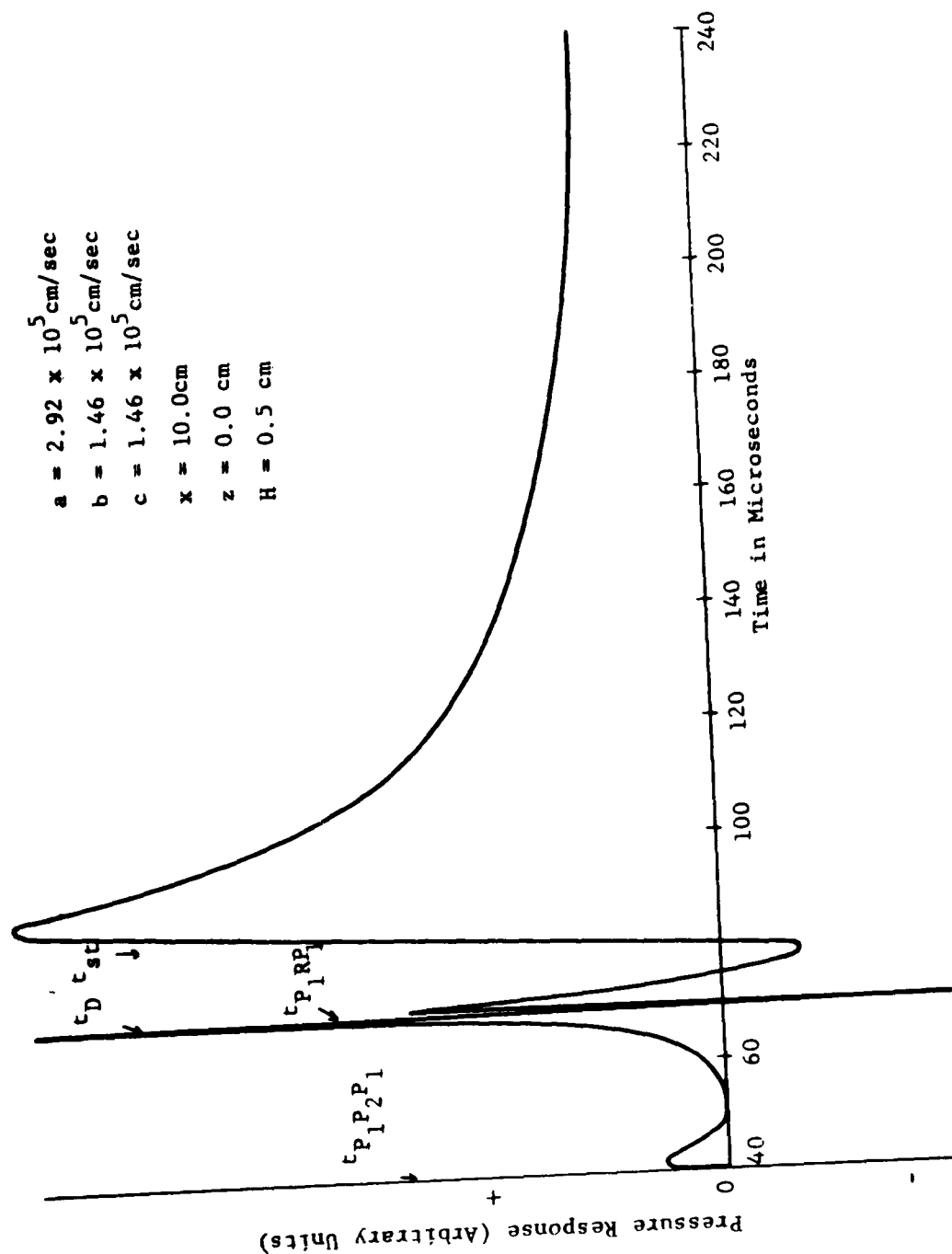


FIGURE 8c. THEORETICAL PRESSURE RESPONSE CURVE FOR A WATER-METAMORPHIC ROCK SYSTEM

4. Extension of the theory to repetitive impulsive sources--This would consist of both theoretical and model work.

5. Consideration of a harmonic type source--If possible, a "point" harmonic type sound source should be obtained and model work done using this source. The theory considered to data should be useful with suitable modification, and an experimental endeavor will prove useful.

6. Investigation of the scale laws governing the various types of waves present in the model work--This would include determination of amplitude decay rates and frequency content changes with varying dimensional parameters.

APPENDIX A

DERIVATION OF THE REFLECTION COEFFICIENTS $A(q)$ AND $N(q)$

Equations (1) and (2) define the 11 displacement potentials considered in this problem. These potentials are subject to the following boundary conditions (See Figure 2):

1. The normal stresses (σ_{zz}) are continuous at $z = H$ and $z = H + J$.
2. The normal displacements (w) are continuous at $z = H$ and $z = H + J$.
3. The tangential stresses (σ_{xz}) are zero at $z = H$ and continuous at $z = H + J$.
4. The tangential displacements (u) are continuous at $z = H + J$.

These boundary conditions give 10 boundary equations which can be used to solve for the 10 quantities $A, B, C, D, E, F, G, I, M$ and N . Hence, instead of the 3 equations and 3 unknowns in the fluid-single solid problem, we now have 10 equations and 10 unknowns. If we had not limited the problem to a maximum of two reflections from the solid-solid interface, even more potentials, and hence unknowns, would have been present.

Since the present problem concerns the response in the fluid, it is only necessary to determine $A(q)$ and $N(q)$.

The displacements and stresses are given by¹:

$$\sigma_{zz}^s = \rho^s \left[\left(1 - 2 \frac{b^2}{a^2} \right) \frac{\partial^2 \phi^s}{\partial t^2} + 2b^2 \left(\frac{\partial^2 \phi^s}{\partial z^2} - \frac{\partial^2 \psi^s}{\partial x \partial z} \right) \right]$$

$$\sigma_{xz}^s = \rho^s \left[\frac{\partial^2 \psi^s}{\partial t^2} + 2b^2 \left(\frac{\partial^2 \phi^s}{\partial x \partial z} - \frac{\partial^2 \psi^s}{\partial x^2} \right) \right]$$

$$\sigma_{zz}^f = \rho^f \left(\frac{\partial^2 \phi^f}{\partial t^2} \right)$$

$$\sigma_{xz}^f = 0$$

$$w^s = \frac{\partial \varphi^s}{\partial z} - \frac{\partial \psi^s}{\partial x}, \quad w^f = \frac{\partial \varphi^f}{\partial z}$$

$$u^s = \frac{\partial \varphi^s}{\partial x} + \frac{\partial \psi^s}{\partial z}$$

Applying the boundary conditions and inserting the displacement potentials (2a - j) into the boundary equations, we obtain:

$$\begin{aligned} A[\rho^f e^{-i\omega\Gamma H}] - B[e^{-i\omega a'H} \rho^s (1 - 2b^2 q^2)] + C[2\rho^s b^2 q b' e^{-i\omega b'H}] \\ = -\rho^f e^{-i\omega\Gamma H} \end{aligned} \quad (A-1)$$

$$A[\Gamma e^{-i\omega\Gamma H}] + B[a' e^{-i\omega a'H}] - C[q e^{-i\omega b'H}] = \Gamma e^{-i\omega\Gamma H} \quad (A-2)$$

$$B[2b^2 a' q e^{-i\omega a'H}] + C[(1 - 2b^2 q^2) e^{-i\omega b'H}] = 0 \quad (A-3)$$

$$\begin{aligned} B[\rho^s (1 - 2b^2 q^2) e^{-i\omega a'(H+J)}] - C[2\rho^s b^2 b' q e^{-i\omega b'(H+J)}] \\ + D[\rho^s (1 - 2b^2 q^2) e^{-i\omega a'(H+J)}] + E[2\rho^s b^2 b' q e^{-i\omega b'(H+J)}] \\ + I[2\rho^s k^2 q k' e^{-i\omega k'(H+J)}] - M[\rho^s (1 - 2k^2 q^2) e^{-i\omega g'(H+J)}] = 0 \end{aligned} \quad (A-4)$$

$$\begin{aligned} B[2\rho^s b^2 a' q e^{-i\omega a'(H+J)}] + C[\rho^s (1 - 2b^2 q^2) e^{-i\omega b'(H+J)}] \\ - D[2\rho^s b^2 a' q e^{-i\omega a'(H+J)}] + E[\rho^s (1 - 2b^2 q^2) e^{-i\omega b'(H+J)}] \\ - I[\rho^s (1 - 2k^2 q^2) e^{-i\omega k'(H+J)}] - M[2\rho^s k^2 g' q e^{-i\omega g'(H+J)}] = 0 \end{aligned} \quad (A-5)$$

$$\begin{aligned}
& - B \left[q e^{-i\omega a' (H + J)} \right] - C \left[b' e^{-i\omega b' (H + J)} \right] - D \left[q e^{-i\omega a' (H + J)} \right] \\
& + E \left[b' e^{-i\omega b' (H + J)} \right] + I \left[k' e^{-i\omega k' (H + J)} \right] + M \left[q e^{-i\omega g' (H + J)} \right] = 0 \quad (A-6)
\end{aligned}$$

$$\begin{aligned}
& - B \left[a' e^{-i\omega a' (H + J)} \right] + C \left[q e^{-i\omega b' (H + J)} \right] + D \left[a' e^{-i\omega a' (H + J)} \right] \\
& + E \left[q e^{-i\omega b' (H + J)} \right] + M \left[g' e^{-i\omega g' (H + J)} \right] - I \left[q e^{-i\omega k' (H + J)} \right] = 0 \quad (A-7)
\end{aligned}$$

$$\begin{aligned}
& D \left[\rho^s 1 (1 - 2b^2 q^2) e^{-i\omega a' (H + 2J)} \right] + E \left[2\rho^s 1 b^2 q b' e^{-i\omega b' (H + 2J)} \right] \\
& + F \left[\rho^s 1 (1 - 2b^2 q^2) e^{-i\omega a' (H + 2J)} \right] - G \left[2\rho^s 1 b^2 q b' e^{-i\omega b' (H + 2J)} \right] \\
& - N \left[\rho^f e^{-i\omega \Gamma (H + 2J)} \right] = 0 \quad (A-8)
\end{aligned}$$

$$\begin{aligned}
& E \left[(1 - 2b^2 q^2) e^{-i\omega b' (H + 2J)} \right] + F \left[2b^2 a' q e^{-i\omega a' (H + 2J)} \right] \\
& + G \left[(1 - 2b^2 q^2) e^{-i\omega b' (H + 2J)} \right] - D \left[2b^2 a' q e^{-i\omega a' (H + 2J)} \right] = 0 \quad (A-9)
\end{aligned}$$

$$\begin{aligned}
& - D \left[a' e^{-i\omega a' (H + 2J)} \right] - E \left[q e^{-i\omega b' (H + 2J)} \right] + F \left[a' e^{-i\omega a' (H + 2J)} \right] \\
& - G \left[q e^{-i\omega b' (H + 2J)} \right] + N \left[\Gamma e^{-i\omega \Gamma (H + 2J)} \right] = 0 \quad (A-10)
\end{aligned}$$

This set of 10 equations can be written very compactly in matrix form:

ρ^f	$-\rho^2(1-2b^2q^2)$	$2\rho^2b^2qb'$	0	0	0	0	0	0	0	0	$A(q)$	$-\rho^f$
Γ	a'	$-q$	0	0	0	0	0	0	0	0	$B(q)$	Γ
0	$2b^2a'q$	$(1-2b^2q^2)$	0	0	0	0	0	0	0	0	$\sim(q)$	0
0	$\rho^2(1-2b^2q^2)e^{-iua'J}$	$-2\rho^2b^2b'qe^{-iubb'J}$	$\rho^2(1-2b^2q^2)$	$\rho^2b^2b'q$	0	0	0	0	$-2\rho^2(1-2k^2q^2)$	0	$D(q)$	0
0	$2\rho^2b^2a'qe^{-iua'J}$	$\rho^2(1-2b^2q^2)e^{-iubb'J}$	$-2\rho^2b^2b'a'q$	$\rho^2(1-2b^2q^2)$	0	0	0	0	$-2\rho^2(1-2k^2q^2)q$	0	$E(q)$	0
0	$-qe^{-iua'J}$	$-b'e^{-iubb'J}$	$-q$	0	0	0	0	0	k'	0	$F(q)$	0
0	$a'e^{-iua'J}$	$qe^{-iubb'J}$	a'	0	0	0	0	0	$-q$	0	$G(q)$	0
0	0	0	$\rho^2(1-2b^2q^2)e^{-iua'J}$	$2\rho^2b^2qb'e^{-iubb'J}$	$\rho^2(1-2b^2q^2)$	$-2\rho^2b^2qb'$	0	0	0	$-\rho^f e^{-2iua'J}$	$I(q)$	0
0	0	0	$-2b^2a'qe^{-iua'J}$	$(1-2b^2q^2)e^{-iubb'J}$	$2b^2a'q$	$(1-2b^2q^2)$	0	0	0	0	$M(q)$	0
0	0	0	$-a'e^{-iua'J}$	$-qe^{-iubb'J}$	a'	$-q$	0	0	0	$\rho^f e^{-2iua'J}$	$N(q)$	0

It is now theoretically possible to solve for each of the 10 unknown quantities by evaluating two 10 by 10 determinants. It should be noted that these determinants immediately reduce to 7 by 7 determinants due to the fact that $A(q)$, $B(q)$, and $C(q)$ are not dependent on the other unknown quantities. Such evaluations will yield equations (3) and (4).

(Reverse Page 54 Blank)

APPENDIX B

THE REFRACTION AND REFLECTION ARRIVALS

It has been shown^{1,2} that in an infinite fluid only a compressional type of wave motion can occur, while in an infinite solid both compressional and shear waves are possible. Considering the liquid-solid interface illustrated in Figure B1, it can be shown that incident compressional waves from the liquid can produce compressional and shear waves in the solid, and also that a surface wave which is tied to the interface can occur. For certain angles of incidence for the impinging energy, critically refracted waves can occur. Furthermore, reflections from the interface are possible. Hence, for this fluid-solid problem, one reflection arrival, two refraction arrivals, one direct arrival, and surface arrivals are predicted.

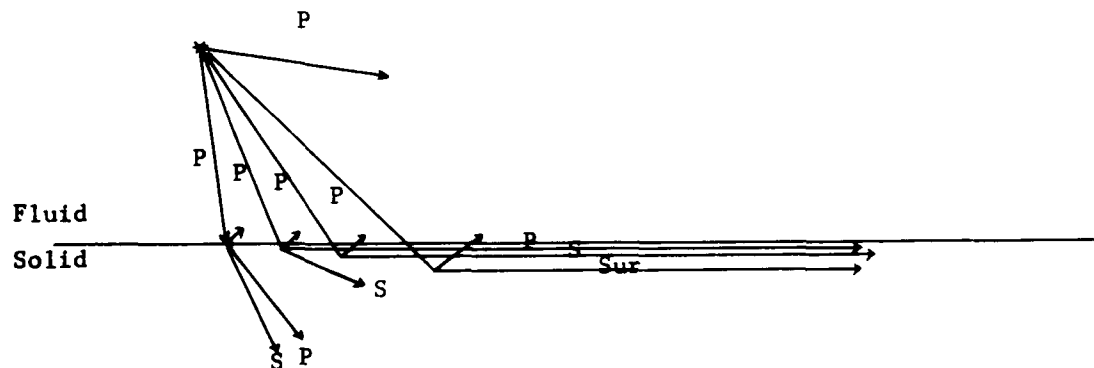


FIGURE B1. THE LIQUID - SOLID INTERFACE

The problem under consideration in this report concerns a fluid overlying a two-layer solid bottom. The prediction of the various reflections and refraction arrivals now becomes much more difficult. In fact, as discussed previously, there are an infinite number of wave arrivals unless a limiting condition is applied to the problem. In the mathematical derivation section of this report the assumption was made that any waves existing after two reflections from the lower (solid-solid) interface could be neglected. As stated previously, this is not always a valid assumption, but for the purpose of this investigation it is acceptable.

Figure B2, B3, B4, and B5 show the ten refraction arrivals that must be considered in the problem.

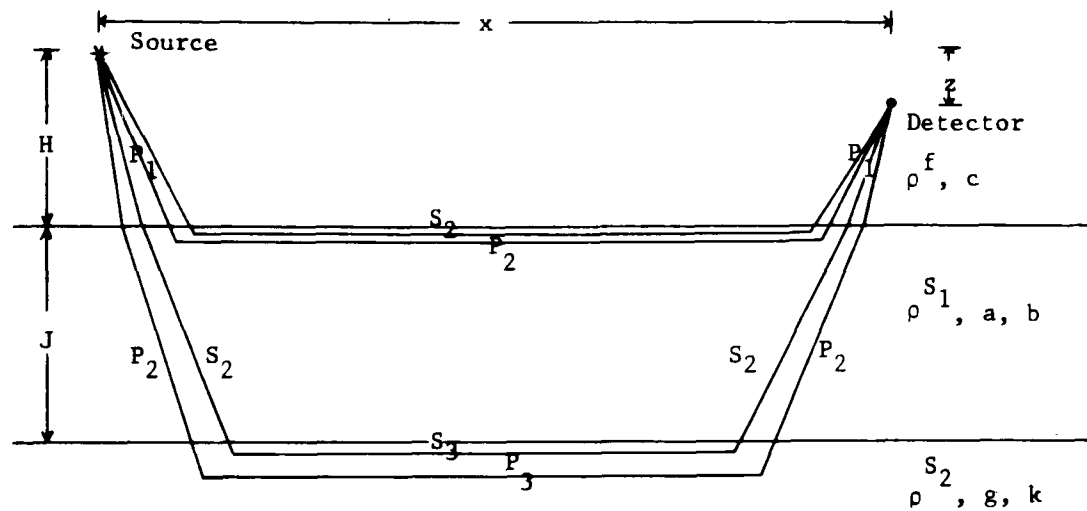


FIGURE B2. THE $P_1 P_2 P_1$, $P_1 S_2 P_1$, $P_1 P_2 P_3 P_2 P_1$, AND $P_1 S_2 S_3 S_2 P_1$ REFRACTION ARRIVALS

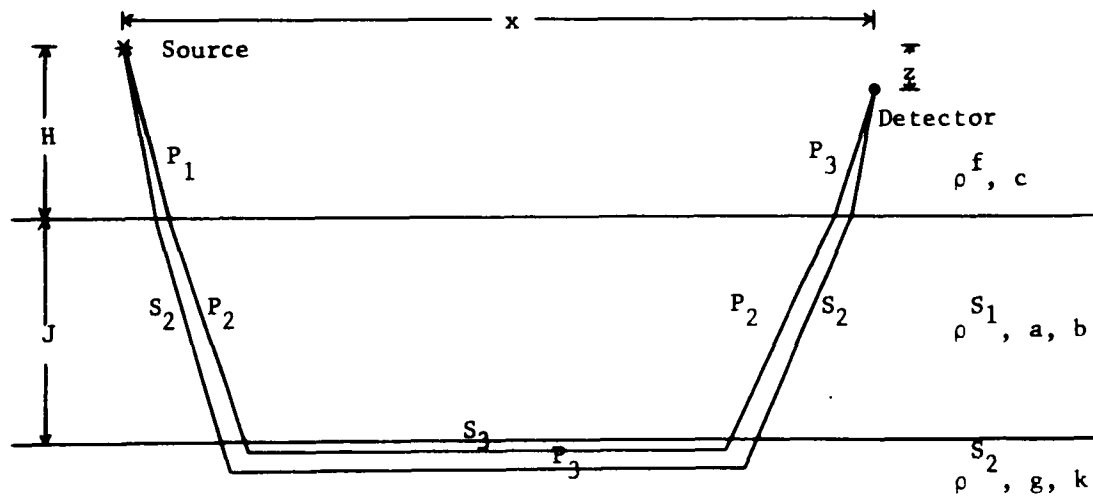


FIGURE B3. THE $P_1 S_2 P_3 S_2 P_1$ AND $P_1 P_2 S_3 P_2 P_1$ REFRACTION ARRIVALS

(Text Continued on Page 58)

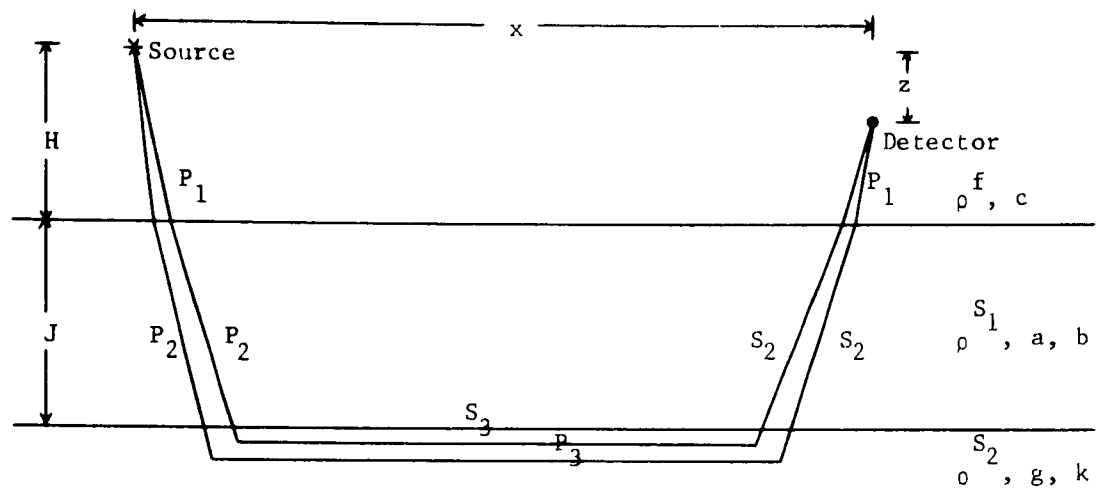


FIGURE B4. THE $P_1P_2P_3S_2P_1$ AND $P_1P_2S_3S_2P_1$ REFRACTION ARRIVALS

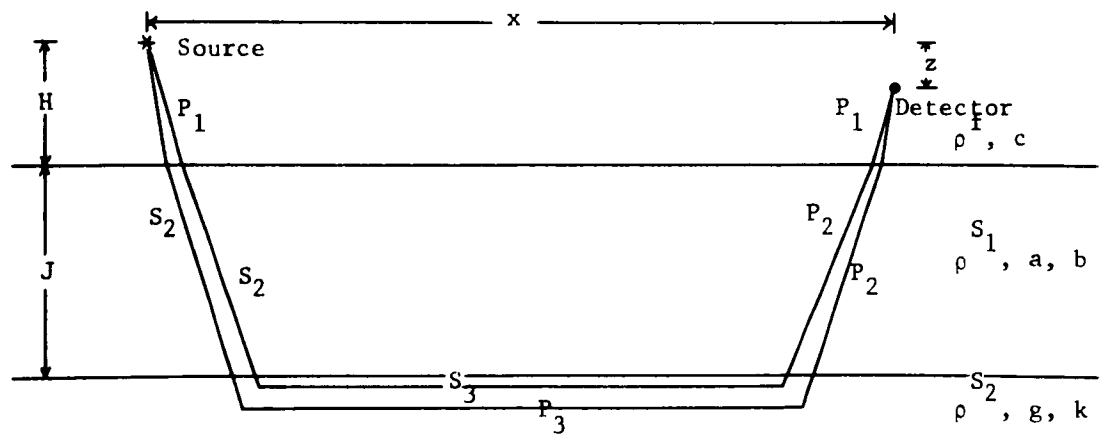


FIGURE B5. THE $P_1S_2P_3P_2P_1$ AND $P_1S_2S_3P_2P_1$ REFRACTION ARRIVAL

Figures B6 and B7 illustrate the five reflection arrivals that must be considered:

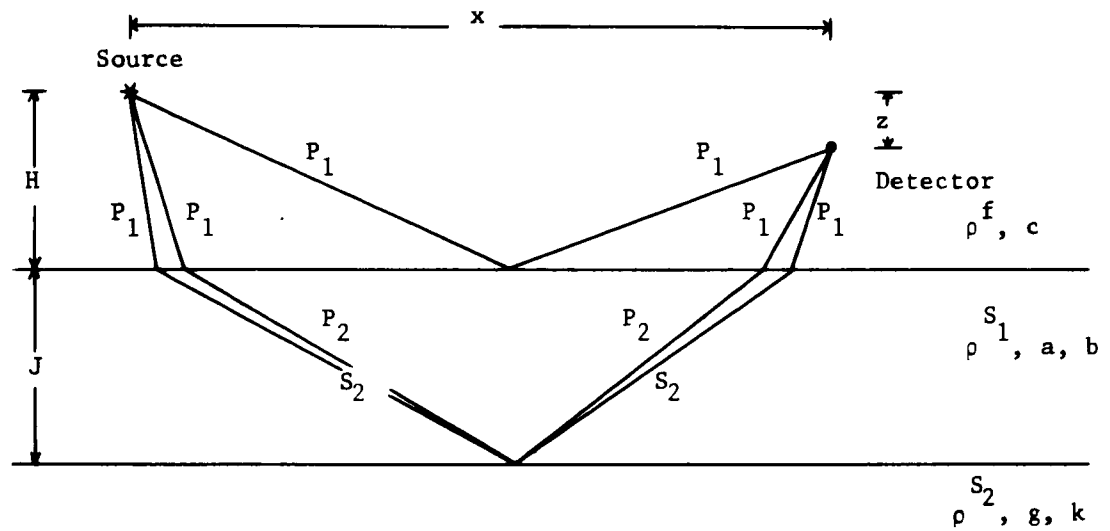


FIGURE B6. THE P_1RP_1 , $P_1P_2RP_2P_1$, AND $P_1S_2RS_2P_1$ REFLECTION ARRIVALS

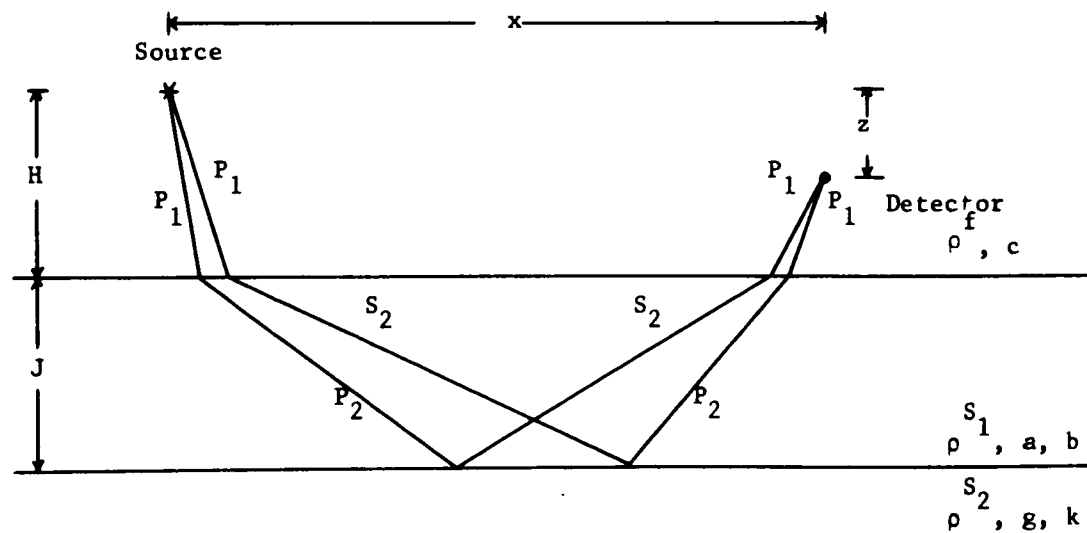


FIGURE B7. THE $P_1P_2RS_2P_1$ AND $P_1S_2RP_2P_1$ REFLECTION ARRIVALS

The two arrivals that are both reflected and critically refracted are shown in Figures B8 and B9.

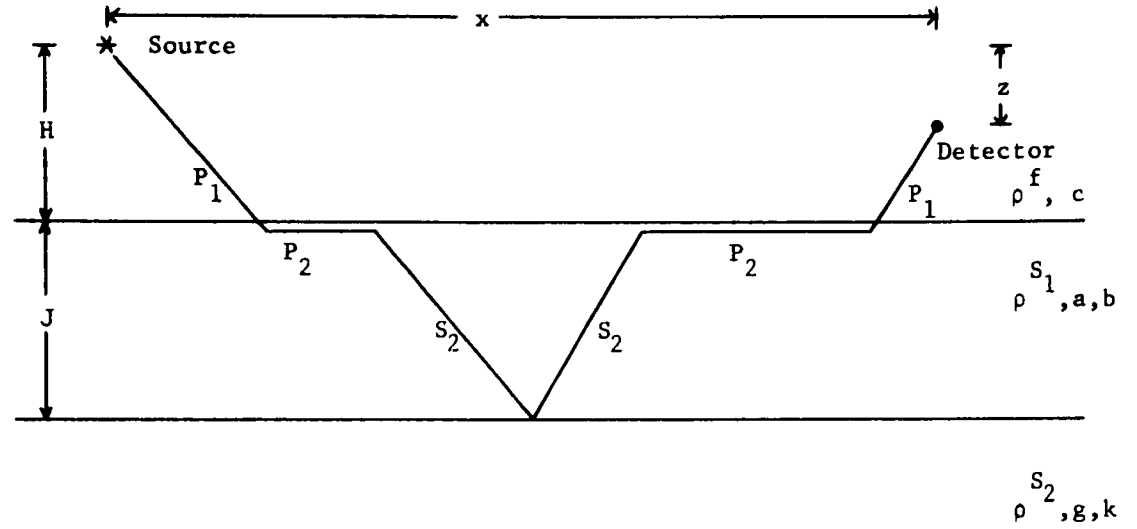


FIGURE B8. THE $P_1P_2S_2RS_2P_2P_1$ REFRACTION - REFLECTION ARRIVAL

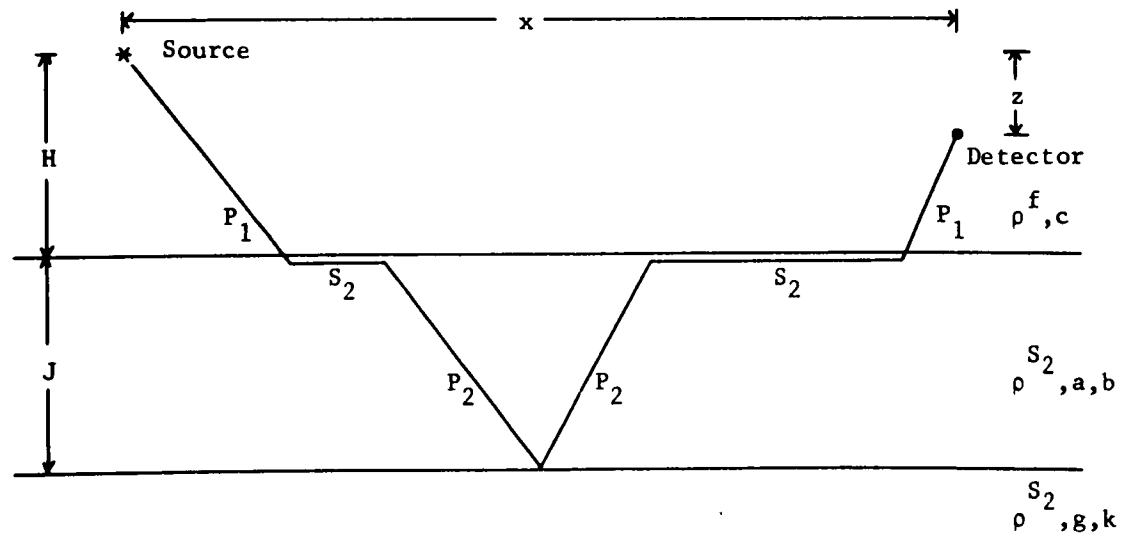


FIGURE B9. THE $P_1S_2P_2RP_2S_2P_1$ REFRACTION - REFLECTION ARRIVAL

Also, we should expect surface or interface waves at both the liquid-solid and solid-solid interfaces, as has been shown previously. Hence, for the assumed liquid-two solid problem, we should expect one direct arrival, ten refraction arrivals, five reflection arrivals, two refraction-reflection arrivals, and the surface arrivals from both interfaces. In other words, there are now over twenty arrivals to analyze, rather than the six arrivals found in the liquid-solid problem.

It has been shown previously¹ that the arrival times for the $P_1P_2P_1$ and $P_1S_2P_1$ refraction arrivals are given by:

$$t_{P_1P_2P_1} = \frac{x}{a} + \frac{2H - z}{c} \left(1 - \frac{c^2}{2a^2}\right)^{\frac{1}{2}} \quad (B-1)$$

and

$$t_{P_1S_2P_1} = \frac{x}{b} + \frac{2H - z}{c} \left(1 - \frac{c^2}{2b^2}\right)^{\frac{1}{2}} \quad (B-2)$$

The derivations of the arrival times of the remaining critically refracted arrivals are similar, so only the $P_1P_2P_3P_2P_1$ expression will be derived and it will be used as a guide to obtain the other arrival times. The symbols used are defined in Figure B10.

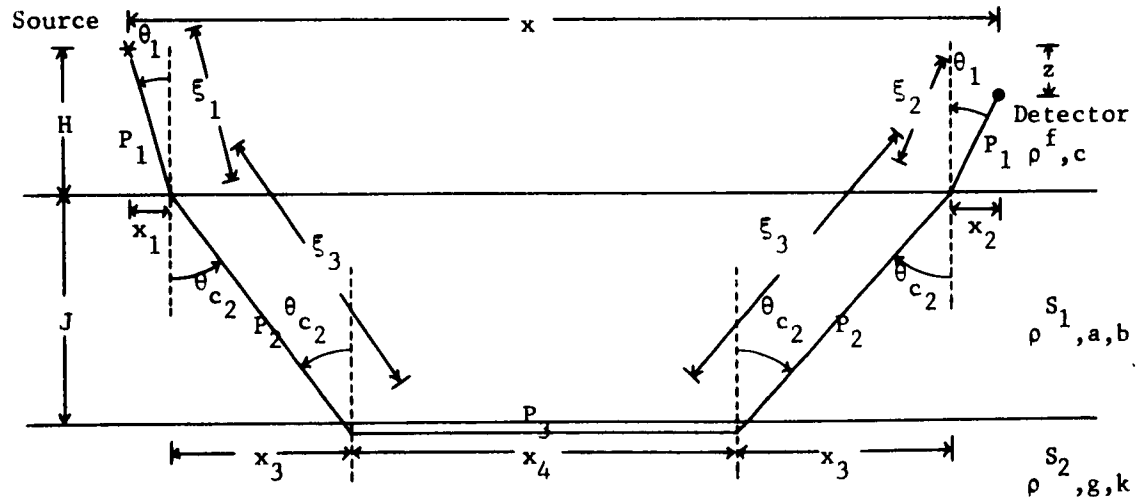


FIGURE B10. DEFINITION OF SYMBOLS FOR THE CALCULATION OF THE
OF THE $P_1P_2P_3P_2P_1$ WAVE

From Snell's law,

$$\frac{\sin \theta_1}{2} = \frac{\sin \theta_{c_2}}{a}, \quad \frac{\sin \theta_{c_2}}{a} = \frac{1}{g}$$

From Figure B10:

$$(\xi_1)^2 = (H)^2 + (x_1)^2$$

$$(\xi_2)^2 = (H - z)^2 + (x_2)^2$$

$$(\xi_3)^2 = (J)^2 + (x_3)^2$$

$$\sin \theta = \frac{x_1}{\xi_1} = \frac{x_2}{\xi_2}$$

$$\sin \theta_{c_2} = \frac{x_3}{\xi_3}$$

Therefore, the travel times in the fluid are given by

$$t_1 = \frac{\xi_1}{c} = \frac{gH}{c(g^2 - c^2)^{\frac{1}{2}}}$$

and

$$t_2 = \frac{\xi_2}{c} = \frac{g(H - z)}{c(g^2 - c^2)^{\frac{1}{2}}}$$

Likewise, the travel times in the upper solid are given by

$$t_3 = \frac{\xi_3}{a} = \frac{Jg}{a(g^2 - a^2)^{\frac{1}{2}}}$$

The travel time in the lower solid is given by

$$t_4 = \frac{x - x_1 - x_2 - 2x_3}{g} = \frac{x}{g} - \frac{(2H - z)c}{g(g^2 - c^2)^{\frac{1}{2}}} - \frac{2aJ}{g(g^2 - a^2)^{\frac{1}{2}}}$$

Therefore, the total travel time for the $P_1P_2P_3P_2P_1$ refraction arrival is given by

$$t_{P_1P_2P_3P_2P_1} = \frac{x}{g} + \frac{(2H - z)}{cg} (g^2 - c^2)^{\frac{1}{2}} + \frac{2J}{ag} (g^2 - a^2)^{\frac{1}{2}} \quad (B-3)$$

The travel time expressions for the other critically refracted arrivals can be found in a manner similar to that used to find $t_{P_1P_2P_3P_2P_1}$. These travel times are given by:

$$t_{P_1S_2S_3S_2P_1} = \frac{x}{k} + \frac{(2H - z)}{ck} (k^2 - c^2)^{\frac{1}{2}} + \frac{2J}{bk} (k^2 - b^2)^{\frac{1}{2}} \quad (A-4)$$

$$t_{P_1S_2P_3S_2P_1} = \frac{x}{g} + \frac{(2H - z)}{cg} (g^2 - c^2)^{\frac{1}{2}} + \frac{2J}{bg} (g^2 - b^2)^{\frac{1}{2}} \quad (A-5)$$

$$t_{P_1P_2S_3P_2P_1} = \frac{x}{k} + \frac{(2H - z)}{ck} (k^2 - c^2)^{\frac{1}{2}} + \frac{2J}{ak} (k^2 - a^2)^{\frac{1}{2}} \quad (A-6)$$

$$t_{P_1P_2P_3S_2P_1} = t_{P_1S_2P_3P_2P_1} = \frac{x}{g} + \frac{(2H - z)(g^2 - c^2)^{\frac{1}{2}}}{gc} + \frac{J}{ag} (g^2 - a^2)^{\frac{1}{2}} + \frac{J}{bg} (g^2 - b^2)^{\frac{1}{2}} \quad (A-7)$$

$$t_{P_1P_2S_3S_2P_1} = t_{P_1S_2S_3P_2P_1} = \frac{x}{k} + \frac{(2H - z)(k^2 - c^2)^{\frac{1}{2}}}{kc} + \frac{J}{ak} (k^2 - a^2)^{\frac{1}{2}} + \frac{J}{bk} (k^2 - b^2)^{\frac{1}{2}} \quad (A-8)$$

The travel time expressions for the reflection arrivals are not as simple as the equations obtained for the refraction arrivals. The geometrical approach necessary to determine the travel times of the reflection arrivals consists of an iterative process. For a given $x, z, H, J, c, a,$ and b , a travel path is found that satisfies Snell's law at each boundary and still passes through the source and detector. Then, once this path is known, it is possible to compute the travel time.

It is possible to obtain an algebraic expression for the travel times of the refraction - reflection arrivals. Figure B11 defines the symbols that will be used in the travel time derivation for the $P_1P_2S_2RS_2P_2P_1$ arrival.

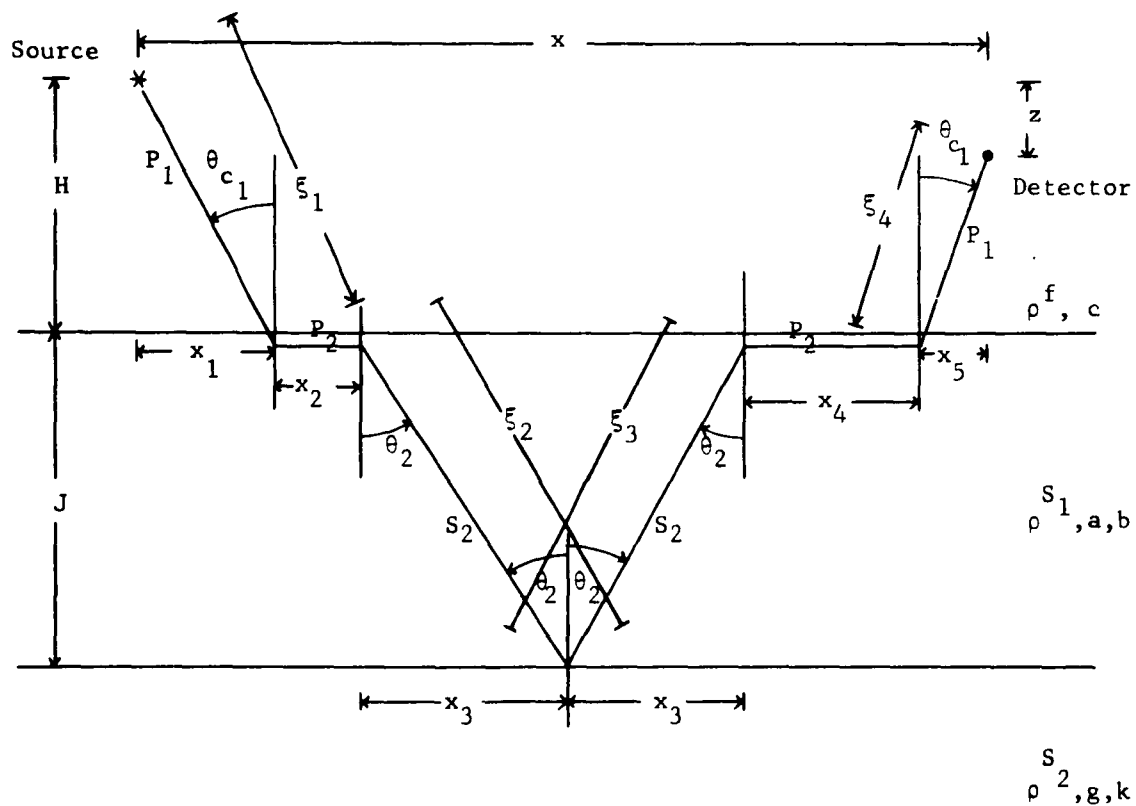


FIGURE B11. DEFINITION OF SYMBOLS FOR THE CALCULATION OF THE ARRIVAL TIME OF THE $P_1P_2S_2RS_2P_2P_1$ ARRIVAL

Snell's law states that:

$$\frac{\sin \theta_{c1}}{c} = \frac{1}{a}, \quad \frac{\sin \theta_2}{b} = \frac{1}{a}$$

From Figure B11:

$$\xi_1^2 = x_1^2 + H^2$$

$$\xi_2^2 = \xi_3^2 = x_3^2 + J^2$$

$$\xi_4^2 = x_5^2 + (H - z)^2$$

$$\sin \theta_{c1} = \frac{x_1}{\xi_1} = \frac{x_5}{\xi_4}$$

$$\sin \theta_2 = \frac{x_3}{\xi_3}$$

Therefore, the travel times in the fluid are given by

$$t_1 = \frac{\xi_1}{c} = \frac{aH}{c(a^2 - c^2)^{\frac{1}{2}}}$$

and

$$t_5 = \frac{\xi_2}{c} = \frac{a(H - z)}{c(a^2 - c^2)^{\frac{1}{2}}}$$

The travel times in the solid are given by

$$2t_3 = \frac{2\xi_3}{b} = \frac{2Ja}{b(a^2 - b^2)^{\frac{1}{2}}}$$

and

$$t_2 + t_4 = \frac{(x_2 + x_4)}{a} = \frac{x}{a} - \frac{c(2H - z)}{a(a^2 - c^2)^{\frac{1}{2}}} - \frac{2bJ}{a(a^2 - b^2)^{\frac{1}{2}}}$$

Thus, the total travel time for the $P_1P_2S_2RS_2P_2P_1$ arrival is given by

$$t = \frac{x}{a} + \frac{(2H - z)}{ac} (a^2 - c^2)^{\frac{1}{2}} + \frac{2J}{ab} (a^2 - b^2)^{\frac{1}{2}} \quad (A-9)$$

Likewise, it can be shown that

$$t_{P_1S_2P_2RP_2S_2P_1} = \frac{x}{b} + \frac{(2H - z)}{bc} (b^2 - c^2)^{\frac{1}{2}} + \frac{2J}{ab} (b^2 - a^2)^{\frac{1}{2}} \quad (A-10)$$

(Reverse Page 66 Blank)

APPENDIX C

EXPERIMENTAL INSTRUMENTATION

The experimental apparatus employed in this project was similar to that used by Roever and Vining in their original verification of Strick's theory.² A detailed description of the apparatus is given in Appendix D of Reference 1. Only a brief description of the apparatus will be included here, along with details of the few modifications necessary in the apparatus to investigate the stratified bottom problem.

The spark source and detection system remains unchanged from the previous work. The spark source consisted of a coaxial spark gap to which was applied the power from a 1 μ f capacitor charged to 812 volts. The peak current during the discharge was over 1000 amperes, and the discharge lasted for about 4 microseconds. The size of the spark gap was about 1 millimeter, so it could be considered to be a point source.

The detector was a Glennite UP-800c ultrasonic probe. This is simply a commercial barium titanate detector designed for minimal disturbance of the sound field. The sensitivity was -153(+1)db (ref: 1v/dyne/cm²) between 10 kc and 400 kc, with good response down to 2 kc and up to 2 mc.

The probe output led to a Tektronic 545 oscilloscope which was triggered by a low-resistance shunt in the discharge circuit. Time resolution was ± 1 microsecond, and was limited by the finite size of the source and detector.

A plaster block (12" x 12" x 10") used in the previous work was also employed in this problem as one of the materials used for the lower semi-infinite solid. A large, solid aluminum cylinder was also used for this purpose. The layer materials used were a 1.27 cm slab of glass and a 3.81 cm slab of plexiglas. The elastic parameters of these materials are given in Table 1.

The question of bonding at the solid interfaces had to be considered carefully. In theoretical derivations the solid-solid interface is considered to be "welded." That is, it is assumed that the tangential stresses and displacements are continuous. Hence, should the solid layers be bonded together, or is it sufficient to simply place them together? A search of the available literature showed about an equal division between the two techniques. A simple solution to the bonding difficulty was as follows:

First, data was obtained for the water - glass - aluminum model with the glass simply lying on the aluminum block. x was 6.5 cm, H was 0.2 cm,

and z was 0.0 cm. Then, the glass and aluminum were bonded with Barge cement and the experiment was repeated. The two sets of data are compared in Figure C1. It can be seen that very little, if any, change occurred because of the bonding of the two materials. Hence, it was concluded that bonding was not necessary in this problem, although if the layer surfaces were not smooth and flat the bonding would probably have been of considerable importance.

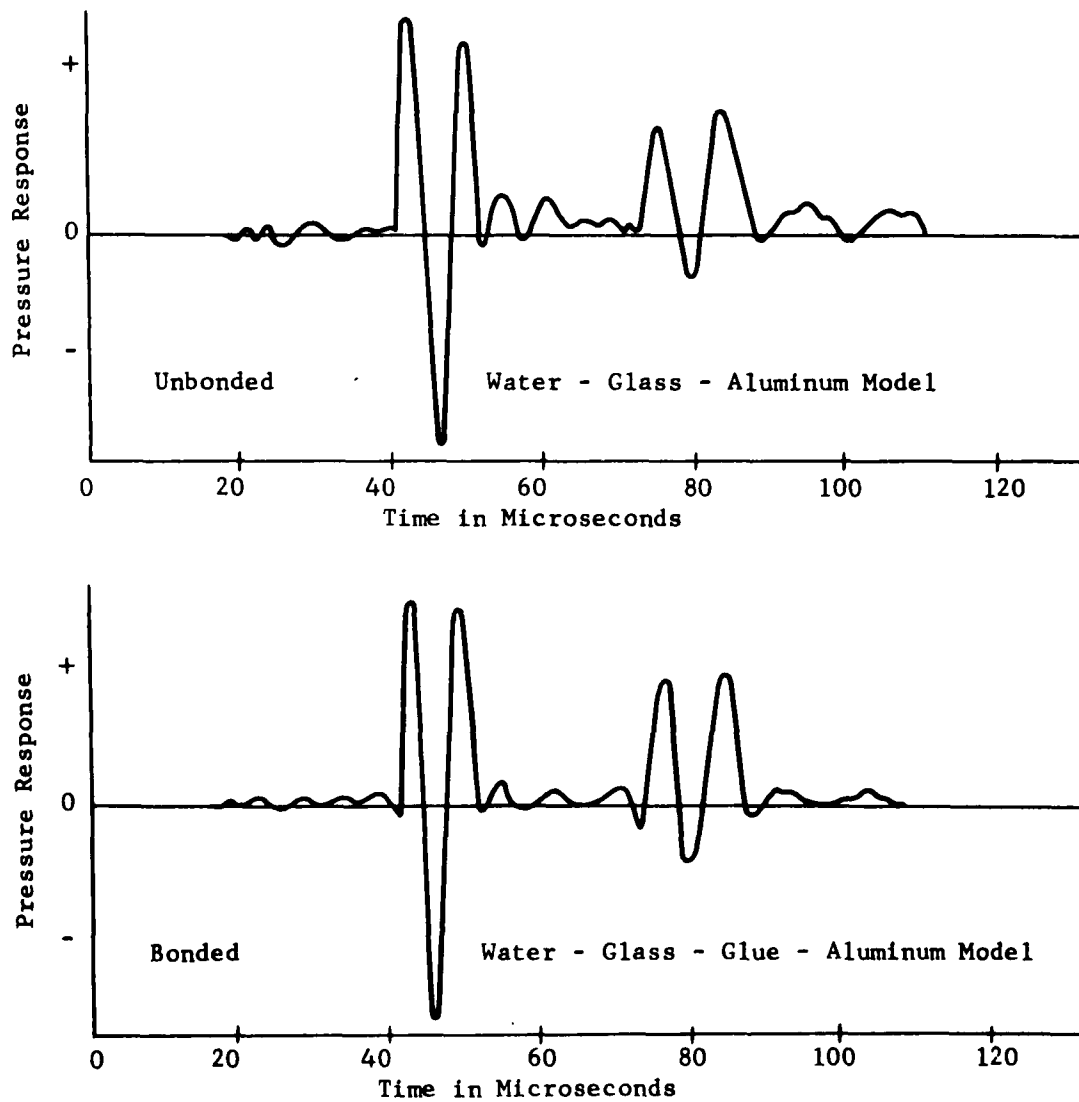


FIGURE C1. ILLUSTRATION OF THE EFFECT OF BONDING THE GLASS AND ALUMINUM LAYERS

REFERENCES

1. Spitznogle, Frank R., "The Propagation at Short Ranges of Elastic Waves from an Impulsive Source at a Liquid-Solid Interface - Fluid-Solid Model," U. S. Navy Mine Defense Laboratory Report 195 (June 1963) UNCLASSIFIED.
2. Strick, E., Roever, W. I., and Vining, T. F., "Propagation of Elastic Wave Motion from an Impulsive Source Along a Fluid - Solid Interface," Philosophical Transactions of the Royal Society of London, Series A, (1959), Vol. 251, pp. 455-523, UNCLASSIFIED.
3. Pekeris, C. L., "Theory of Propagation of Explosive Sounds in Shallow Water," Propagation of Sound in the Ocean, Mem. No. 27, Geological Society of America, (1948) UNCLASSIFIED.
4. Officer, C. B., "Normal Mode Propagation in a Three Layered Liquid Half-Space by Ray Theory," Geophysics, Vol. 16 (1951), pp. 207-212, UNCLASSIFIED.
5. Press, F., and Ewing, W. M., "Low Speed Layer in Water Covered Areas," Geophysics, Vol. 13, (1948), pp. 404-420, UNCLASSIFIED.
6. McLeroy, E. G., "Complex Image Theory of Low-Frequency Sound Propagation in Shallow Water," Journal of the Acoustical Society of America, Vol. 33, UNCLASSIFIED.
7. Strick, E., and Ginzburg, A. S., "Stoneley - Wave Velocities for a Fluid-Solid Interface," Bulletin of the Seismological Society of America, (1956) Vol. 46, pp. 281-292, UNCLASSIFIED.
8. Stoneley, R., "Elastic Waves at the Surface of Separation of Two Solids," Proceedings of the Royal Society of London, Series A, (1924), Vol. 106, pp. 416-428, UNCLASSIFIED.
9. Scholte, J. G., "The Range of Existence of Rayleigh and Stoneley Waves," Monthly Notices of the Royal Astronomical Society, Geophysics Supplement, (1947), Vol. 5, pp. 120-126, UNCLASSIFIED.
10. Ewing, W. M., Jardetzky, W. S., and Press, F., Elastic Waves in Layered Media, McGraw-Hill, (1957), UNCLASSIFIED.

<p>Navy Mine Defense Laboratory. Report 206. THE PROPAGATION AT SHORT RANGES OF ELASTIC WAVES FROM AN IMPULSIVE SOURCE AT A LIQUID-SOLID INTERFACE - THE FLUID-TWO LAYER SOLID SYSTEM by Frank R. Spitznogle. August 1963. 69 p., illus. UNCLASSIFIED</p> <p>References: 10 refs. This report consists of an extension to a system of a fluid layer and two underlying solid layers, of a theory recently published by Strick which concerns the prediction of the pressure field produced at short ranges by an impulsive sound source near a fluid-homogeneous solid interface. The theoretical extension should prove useful in permitting the prediction of the pressure field at close ranges produced by a low-frequency sound source lying near the ocean floor. Although the final</p> <p>(over)</p>	<p>1. Underwater sound - Propagation 2. Underwater sound reflection - Mathematical analysis 3. Ocean bottom - Sound transmission I. Spitznogle, Frank R. II. Title III. FUST 19 IV. SF 011 01 01 V. Task 2612</p> <p>UNCLASSIFIED</p>	<p>1. Underwater sound - Propagation 2. Underwater sound reflection - Mathematical analysis 3. Ocean bottom - Sound transmission I. Spitznogle, Frank R. II. Title III. FUST 19 IV. SF 011 01 01 V. Task 2612</p> <p>UNCLASSIFIED</p>
<p>Navy Mine Defense Laboratory. Report 206. THE PROPAGATION AT SHORT RANGES OF ELASTIC WAVES FROM AN IMPULSIVE SOURCE AT A LIQUID-SOLID INTERFACE - THE FLUID-TWO LAYER SOLID SYSTEM by Frank R. Spitznogle. August 1963. 69 p., illus. UNCLASSIFIED</p> <p>References: 10 refs. This report consists of an extension to a system of a fluid layer and two underlying solid layers, of a theory recently published by Strick which concerns the prediction of the pressure field produced at short ranges by an impulsive sound source near a fluid-homogeneous solid interface. The theoretical extension should prove useful in permitting the prediction of the pressure field at close ranges produced by a low-frequency sound source lying near the ocean floor. Although the final</p> <p>(over)</p>	<p>1. Underwater sound - Propagation 2. Underwater sound reflection - Mathematical analysis 3. Ocean bottom - Sound transmission I. Spitznogle, Frank R. II. Title III. FUST 19 IV. SF 011 01 01 V. Task 2612</p> <p>UNCLASSIFIED</p>	<p>1. Underwater sound - Propagation 2. Underwater sound reflection - Mathematical analysis 3. Ocean bottom - Sound transmission I. Spitznogle, Frank R. II. Title III. FUST 19 IV. SF 011 01 01 V. Task 2612</p> <p>UNCLASSIFIED</p>

form of the extended theory is not obtained in closed form, it can predict all arrivals at short ranges. It is concluded that the existence of Stoneley waves at a solid-solid interface is unlikely, although reflections from the solid-solid interface may be responsible for the formation of additional Stoneley waves at the fluid-solid interface.

UNCLASSIFIED

form of the extended theory is not obtained in closed form, it can predict all arrivals at short ranges. It is concluded that the existence of Stoneley waves at a solid-solid interface is unlikely, although reflections from the solid-solid interface may be responsible for the formation of additional Stoneley waves at the fluid-solid interface.

UNCLASSIFIED

form of the extended theory is not obtained in closed form, it can predict all arrivals at short ranges. It is concluded that the existence of Stoneley waves at a solid-solid interface is unlikely, although reflections from the solid-solid interface may be responsible for the formation of additional Stoneley waves at the fluid-solid interface.

UNCLASSIFIED

form of the extended theory is not obtained in closed form, it can predict all arrivals at short ranges. It is concluded that the existence of Stoneley waves at a solid-solid interface is unlikely, although reflections from the solid-solid interface may be responsible for the formation of additional Stoneley waves at the fluid-solid interface.

UNCLASSIFIED

<p>Navy Mine Defense Laboratory. Report 206. THE PROPAGATION AT SHORT RANGES OF ELASTIC WAVES FROM AN IMPULSIVE SOURCE AT A LIQUID-SOLID INTERFACE - THE FLUID-TWO LAYER SOLID SYSTEM by Frank R. Spitznogle. August 1963. 69 p., illus. UNCLASSIFIED</p> <p>References: 10 refs. This report consists of an extension to a system of a fluid layer and two underlying solid layers, of a theory recently published by Strick which concerns the pre- diction of the pressure field produced at short ranges by an impulsive sound source near a fluid-homogeneous solid interface. The theoretical extension should prove useful in permitting the prediction of the pressure field at close ranges produced by a low-frequency sound source lying near the ocean floor. Although the final</p> <p>(over)</p>	<p>1. Underwater sound - Propagation 2. Underwater sound reflection - 2 Mathematical analysis 3. Ocean bottom - Sound transmission I. Spitznogle, Frank R. II. Title III. FUST 19 IV. SF 011 01 01 V. Task 2612</p> <p>UNCLASSIFIED</p>	<p>Navy Mine Defense Laboratory. Report 206. THE PROPAGATION AT SHORT RANGES OF ELASTIC WAVES FROM AN IMPULSIVE SOURCE AT A LIQUID-SOLID INTERFACE - THE FLUID-TWO LAYER SOLID SYSTEM by Frank R. Spitznogle. August 1963. 69 p., illus. UNCLASSIFIED</p> <p>References: 10 refs. This report consists of an extension to a system of a fluid layer and two underlying solid layers, of a theory recently published by Strick which concerns the pre- diction of the pressure field produced at short ranges by an impulsive sound source near a fluid-homogeneous solid interface. The theoretical extension should prove useful in permitting the prediction of the pressure field at close ranges produced by a low-frequency sound source lying near the ocean floor. Although the final</p> <p>(over)</p> <p>1. Underwater sound - Propagation 2. Underwater sound reflection - 2 Mathematical analysis 3. Ocean bottom - Sound transmission I. Spitznogle, Frank R. II. Title III. FUST 19 IV. SF 011 01 01 V. Task 2612</p> <p>UNCLASSIFIED</p>
<p>Navy Mine Defense Laboratory. Report 206. THE PROPAGATION AT SHORT RANGES OF ELASTIC WAVES FROM AN IMPULSIVE SOURCE AT A LIQUID-SOLID INTERFACE - THE FLUID-TWO LAYER SOLID SYSTEM by Frank R. Spitznogle. August 1963. 69 p., illus. UNCLASSIFIED</p> <p>References: 10 refs. This report consists of an extension to a system of a fluid layer and two underlying solid layers, of a theory recently published by Strick which concerns the pre- diction of the pressure field produced at short ranges by an impulsive sound source near a fluid-homogeneous solid interface. The theoretical extension should prove useful in permitting the prediction of the pressure field at close ranges produced by a low-frequency sound source lying near the ocean floor. Although the final</p> <p>(over)</p>	<p>1. Underwater sound - Propagation 2. Underwater sound reflection - 2 Mathematical analysis 3. Ocean bottom - Sound transmission I. Spitznogle, Frank R. II. Title III. FUST 19 IV. SF 011 01 01 V. Task 2612</p> <p>UNCLASSIFIED</p>	<p>Navy Mine Defense Laboratory. Report 206. THE PROPAGATION AT SHORT RANGES OF ELASTIC WAVES FROM AN IMPULSIVE SOURCE AT A LIQUID-SOLID INTERFACE - THE FLUID-TWO LAYER SOLID SYSTEM by Frank R. Spitznogle. August 1963. 69 p., illus. UNCLASSIFIED</p> <p>References: 10 refs. This report consists of an extension to a system of a fluid layer and two underlying solid layers, of a theory recently published by Strick which concerns the pre- diction of the pressure field produced at short ranges by an impulsive sound source near a fluid-homogeneous solid interface. The theoretical extension should prove useful in permitting the prediction of the pressure field at close ranges produced by a low-frequency sound source lying near the ocean floor. Although the final</p> <p>(over)</p> <p>1. Underwater sound - Propagation 2. Underwater sound reflection - 2 Mathematical analysis 3. Ocean bottom - Sound transmission I. Spitznogle, Frank R. II. Title III. FUST 19 IV. SF 011 01 01 V. Task 2612</p> <p>UNCLASSIFIED</p>

form of the extended theory is not obtained in closed form, it can predict all arrivals at short ranges. It is concluded that the existence of Stoneley waves at a solid-solid interface is unlikely, although reflections from the solid-solid interface may be responsible for the formation of additional Stoneley waves at the fluid-solid interface.

UNCLASSIFIED

form of the extended theory is not obtained in closed form, it can predict all arrivals at short ranges. It is concluded that the existence of Stoneley waves at a solid-solid interface is unlikely, although reflections from the solid-solid interface may be responsible for the formation of additional Stoneley waves at the fluid-solid interface.

UNCLASSIFIED

form of the extended theory is not obtained in closed form, it can predict all arrivals at short ranges. It is concluded that the existence of Stoneley waves at a solid-solid interface is unlikely, although reflections from the solid-solid interface may be responsible for the formation of additional Stoneley waves at the fluid-solid interface.

UNCLASSIFIED

form of the extended theory is not obtained in closed form, it can predict all arrivals at short ranges. It is concluded that the existence of Stoneley waves at a solid-solid interface is unlikely, although reflections from the solid-solid interface may be responsible for the formation of additional Stoneley waves at the fluid-solid interface.

UNCLASSIFIED

UNCLASSIFIED

UNCLASSIFIED